

Article

Effect of Aggregate on the Performance of Fly-Ash-Based Geopolymer Concrete

Ahmad B. Malkawi 

Civil Engineering Department, Faculty of Engineering Technology, Al-Balqa Applied University, Amman 11134, Jordan; abmalkawi@bau.edu.jo

Abstract: The influence of geopolymer binder characteristics on the performance of geopolymer concrete has been extensively investigated. Yet, the influence of aggregate properties has not been thoroughly studied, and it is usually assumed that their effect is the same as in cement concrete. This study investigates the effect of aggregate on the performance of fly-ash-based geopolymer concrete. A systematic experimental study was undertaken to investigate the effect of aggregate parameters, including volume fractions (AVFs), coarse aggregate to the total aggregate ratio (CAR), maximum coarse aggregate size (MAS), and fineness modulus of fine aggregate (FFM) on the compressive strength, slump, apparent volume of permeable pores (AVPPs), and the air content of geopolymer concrete. Response surface methodology (RSM) using the central composite design approach was utilized to design the experiments and analyze the results statistically. The analysis shows that all of the investigated aggregate parameters have significant first-order effects on the measured properties. No significant interaction between any of the investigated parameters was found. The aggregate may alter the geopolymerization processes, whereby SEM-EDS analysis revealed statistically significant variations in the elemental concentrations of the produced paste as the aggregate parameters changed. Quantitative weights were assigned to the effect of the investigated aggregate parameters on the measured properties. Multi-objective optimization was carried out to obtain the best combinations of the investigated parameters. Additionally, the developed contour graphs may provide an effective tool that can be used as a guide in establishing the first trial mixtures. A wide range of consistencies (10–210 mm slump) and compressive strengths (15–55 MPa) can be obtained by controlling the aggregate grading and proportions.



Citation: Malkawi, A.B. Effect of Aggregate on the Performance of Fly-Ash-Based Geopolymer Concrete. *Buildings* **2023**, *13*, 769. <https://doi.org/10.3390/buildings13030769>

Academic Editor: Moncef L. Nehdi

Received: 19 February 2023

Revised: 6 March 2023

Accepted: 9 March 2023

Published: 15 March 2023



Copyright: © 2023 by the author. Licensee MDPI, Basel, Switzerland. This article is an open access article distributed under the terms and conditions of the Creative Commons Attribution (CC BY) license (<https://creativecommons.org/licenses/by/4.0/>).

Keywords: geopolymer; concrete; aggregate; compressive strength; workability; air content; porosity; response surface; optimization

1. Introduction

Environmental sustainability is one of the major domains that receives increasing global attention. Environmental sustainability aims to maintain natural resources and ecosystems to ensure the needs and well-being of future generations [1]. Environmental sustainability must be understood not as an option, but as a necessity. Unhealthy environments (avoidable environmental risk factors) are responsible for about a quarter of deaths around the world, as estimated by the World Health Organization [2]. Generations born in 1960 and earlier have clearly witnessed climate changes during the last 50 years, including extreme heat, varying rainfall patterns, and natural disasters. These climate changes are directly related to the human carbon dioxide footprint, mainly from the combustion of fossil fuels and their related industries. It is expected that climate change will be responsible for about 250,000 additional deaths annually between 2030 and 2050 [2]. The cement industry is one of the major carbon dioxide producers, with the production of each ton of cement emitting around 1 ton of greenhouse gases [3]. By observing the global cement production rate, which was around 1.39 billion tons in 1995 and became around 4.1 billion tons in 2020 [4], one can realize the extent to which the construction

industry has grown since then. The construction industry has become one of the major consumers of renewable and non-renewable natural resources and environment-polluting industries [5]. The development of new green construction materials has become a global need and a driver for recent research trends [6]. On the other hand, recycling and waste disposal strategies are of great interest in sustainability issues. Geopolymer binders are a promising solution for the aforementioned issues. Geopolymeric binders are initiated by the reaction of a certain alkaline solution with aluminosilicate-rich source materials, such as fly ash or ground-granulated blast furnace sludge [7]. The use of geopolymer binders can reduce the consumption of ordinary cement and utilize several wastes that are usually dumped in landfills, causing several environmental issues.

Geopolymer concrete investigations so far have demonstrated its superior properties as a promising construction material [8,9]. The main parameters that control geopolymeric binder properties, including source material characteristics, alkaline activator properties, mixing proportions of source material and alkaline activator, and curing conditions, have been thoroughly investigated [10–12]. These parameters are the main variables controlling the properties of the geopolymeric binder itself. On the other hand, geopolymer concrete should be viewed as a two-phase material involving the binder phase and aggregate phase. The aggregate phase consists of fine and coarse aggregates and occupies the highest percentage of the geopolymer concrete total volume. Yet, limited attention has been paid to the influence of aggregate on geopolymer concrete properties. Parameters including aggregate volume fractions, coarse and fine aggregate grading and their mixing proportions, aggregate type and its reactivity in a geopolymer binder, the bonding of aggregate and geopolymeric matrix, interfacial transition zone density, and microstructure properties should all be widely studied to pave the road for geopolymer concrete acceptance in the real-world construction industry.

In ordinary cement concrete, it is usually assumed that the aggregate is a chemically inert filler that does not interact with the cement hydration reactions [13]. In the case of geopolymer concrete, it has been reported that the reactivity of sand aggregate plays a significant role in the formation of geopolymeric binders and their properties as the geopolymerization processes have different mechanisms to cement hydration reactions [14]. It has been suggested that there is an optimum surface area of sand aggregate at which a higher geopolymerization rate would be achieved by increasing the leachability of the aluminosilicate precursors. Moreover, the finer the sand particles, the higher the strength development rate obtained [15]. The compressive strength increased by more than 65% for the geopolymer with silicate and quartz particles compared to the geopolymer with silicate alone [16]. On the other hand, the overall mixture performance and mechanical properties of the produced concrete are functions of aggregate properties, especially the coarse aggregate. Aggregate gradation and shape mainly specify the packing of the aggregate. The dense packing of the aggregate may reduce the amount of the geopolymer binder layer coating the particles; therefore, the mixture's workability will be reduced [17]. At the same time, reducing the amount of geopolymer binder is required to reduce the cost of the produced concrete. Hence, there will be an optimum aggregate content and gradation at which the design requirements could be met.

Aggregate may yield different effects on geopolymer concrete's fresh and hardened properties as compared to ordinary cement concrete. This is due to the nature of the viscous alkaline solution and geopolymeric network structure. Many researchers have highlighted the superior bonding properties between the geopolymer binders and the aggregate. The interfacial transition zone (ITZ) between the geopolymer binder and aggregate was not observed in some types of geopolymer concrete [18,19]. The geopolymer binder can strongly adhere to the aggregate surface, which can be attributed to the unique three-dimensional matrix of the geopolymeric gel [12]. The microstructure and the better physical–chemical properties of the geopolymeric binder (as compared to cement concrete) produce denser and fewer intrinsic defects in the ITZ [20]. This improvement in the ITZ may make geopolymer concrete more affected by the aggregate mechanical properties, which may be similar to

the case of high-strength cement concrete [21]. In normal-strength cement concrete, most of the normal-weight aggregate has a strength much greater than the paste strength, and the ITZ strength creates upper limits on the achieved compressive strength [22]. Therefore, the role that aggregate plays in geopolymer concrete should be emphasized to ensure satisfactory performance. At present, there is no rational relationship that permits the prediction of geopolymer concrete strength based on the binder and aggregate variables. In ordinary cement concrete, it was reported that increasing the aggregate volume fraction will reduce the compressive strength of concrete, and a plateau will be reached at a value of 0.5 [23]. The strength of cement concrete is largely influenced by coarse aggregate properties, while fine aggregate shows a smaller effect due to its influence on the amount of required water [22]. This behavior may differ in the case of geopolymer concrete which has different rheological behavior [24]. Over the last two decades, many researchers have attempted to develop standard procedures for geopolymer concrete mix design mainly based on a trial-and-error approach. However, the number of variables associated with geopolymer concrete production complicates this task. Investigating the effect of all parameters at once will be a challenging task. By looking at geopolymer concrete as a two-phase material composed of the geopolymer binder phase and aggregate phase, it would be necessary to first understand the characteristics of each phase and then develop the mixture relationship. In addition, applying the design of experiment techniques may provide an effective tool that could minimize the required efforts [25].

The effects of aggregate properties on geopolymer concrete performance remain poorly understood (as evidenced by the contradictory results discussed in Section 2 below). To the best of the author's knowledge, no formal studies have been conducted to investigate the effects of aggregate-related parameters on geopolymer concrete performance. The available studies are limited to only a few properties of the aggregate and they usually disregard their effect on the air content and porosity of geopolymer concrete. The significance of this study is that it investigates all of the parameters related to aggregate grading and proportions over a wide range. This study also investigates the interaction effect of the investigated parameters using RSM and quantifies their weights. The conducted microstructural analysis will contribute to the understanding of the aggregate's impact on geopolymer concrete performance. The new findings of this study, along with the presented comprehensive literature review, will provide a new perspective on the aggregate's role in geopolymer concrete performance. The study shows that even though the aggregate is considered to be an inert component of concrete, it can affect the properties of the produced geopolymer binder. Additionally, the study provides contour graphs that can be used as a first step in generating an initial mix design of geopolymer concrete. The conducted optimization for the aggregate content, size, and grading can be used to control the mixture's workability, strength, dimensional stability, and economy.

2. Background on the Effect of Aggregate on Geopolymer Concrete

Geopolymer binders can be produced using any rich aluminosilicate source material [12]. Fly-ash- and slag-based geopolymers are the most common in use due to their high aluminosilicate content and availability [26,27]. For the alkaline activator, sodium silicate and sodium hydroxide solutions have been regularly used in geopolymer binder production due to their low cost compared to other possible alkaline activators [12,26]. The following sections consider the production of geopolymer concrete based on fly ash as the source material and a mixture of sodium silicate and sodium hydroxide solutions as the activating solution unless specified otherwise. The discussion mainly focuses on the effect of aggregate on geopolymer concrete properties, as this is the main topic of this paper.

The literature was collected from two databases: Web of Science and ScienceDirect. Among the collected literature, few studies have solely considered the effect of aggregate parameters on the properties of geopolymer concrete. Previous evaluations of the aggregate influence on geopolymer concrete properties have indirectly considered the aggregate effect (not as the main variable), and only a few aggregate parameters have been involved.

By searching for the keywords “Geopolymer” and “Aggregate” or “Mix Design” in the Title field, most found publications were seen to have considered the use of recycled or manufactured geopolymer aggregate [28–30], the effects of aggregate type [31], biomass aggregate [32], lightweight aggregate [33–35], the alkali–silica reaction of aggregate [36], and mix design studies that have considered the factors affecting the geopolymer paste [37], geopolymer mortars [38], or rigid pavement mix design [39]. Other studies investigated the different types of geopolymer concrete, including lightweight [40], foam [41], and fiber-reinforced [42]. Some studies considered the effect of aggregate on compressive strength and neglected its effect on workability. Nevertheless, a good mix design cannot overlook the workability requirements.

The effect of fine aggregate content and grading on the mechanical properties of geopolymer mortars has been investigated by many researchers. For the metakaolin-based geopolymer, the compressive strength decreased slightly when the content of silica sand (size in the range of 0.3–0.6 mm) increased up to 50 V.%. Any further increment resulted in a sharp strength reduction [43]. Similar observations were reported by Arellano-Aguilar et al. [44] where the compressive strength decreased by more than 60% when the fine limestone content increased from 75 to 88 V.%. The addition of fine aggregate induces the formation of the pores, and a high content will increase the pore radius dramatically which can correspond to the strength reduction [43]. However, the slight strength reduction at a lower content can be attributed to the formation of combinations on the surface of particles which prompts their incorporation within the geopolymeric matrix.

NMR measurements show that more tetrahedral silicon forms when sand or limestone is added to the geopolymeric binder. This is due to the surface dissolution of the small particle sizes less than 75 μm [43,44]. Large-sized aggregate particles will not show significant combination formation. Similar observations were reported by Isabella et al. [15], where a higher rate of silicon dissolution from the sand particles was reported for the particles of higher surface areas.

The grading of fine particles also affects the strength and workability of geopolymer mortars. Larger fine particles (in the range of 2–4 mm) tend to provide higher mortar flowability and strength [45]. A recent investigation devoted to studying the effect of sand gradation and content on geopolymer mortar properties revealed that good mechanical performance can be achieved when the water–binder ratio and sand–binder ratio are in the range of 0.35–0.4 and 0.5–0.65, respectively. The flowability of mortars was directly proportionated to the fineness modulus of the fine aggregate in a linear fashion. The same effect was observed for compressive and flexural strengths. On the other hand, an optimum fineness modulus in the range of 2.2–2.6 resulted in the highest brittleness index and tensile strength [46]. Another study by Furkan et al. focused on the effect of the fine aggregate type, whereby six types of aggregate were investigated. The highest flexural and compressive strengths were obtained using basalt sand followed by silica sand, sandstone, river sand, Rilem sand, and waste concrete aggregate, respectively. Parallel results were obtained in terms of workability [47]. Some researchers were also interested in finding the optimum blend of different types of fine aggregates, such as granite slurry and sand [48], and limestone and sand [45].

Good efforts have been made to understand the physical and chemical characteristics of the interfacial transition zone between the geopolymer binder and aggregate. A uniform and dense interfacial zone has been reported by many researchers independently on the type of aggregate [8,49]. No obvious distinction was noticed between the ITZ microstructure and the bulk of the geopolymeric matrix. This can be attributed to the better chemical interaction between the aggregate and the geopolymeric binders [50,51].

The fly ash content was reported to insignificantly affect the compressive strength of the geopolymer concrete if reasonable content was used [52]. It was suggested that a weak bond exists between unreacted fly ash particles and the binder matrix itself. Hence, the greater amounts of fly ash reduced the geopolymer concrete strength. This could be reasonable only if the fly ash content increased without increasing the alkaline solution.

However, at a constant alkaline solution to fly ash ratio, the amount of the produced gel will increase [53].

A study by Olivia and Nikraz [26] investigated the effect of total aggregate content which varied between 75 and 79 Wt.% on the durability of geopolymer concrete in a sea water environment. The results showed that the aggregate content had the highest response index as compared to the other investigated parameters, including the ratio of the alkaline solution to fly ash, the sodium silicate/sodium hydroxide ratio, and the curing conditions. The highest compressive strength was also achieved at the highest aggregate content. An opposite trend was also reported in the literature [54]. In this study, the investigated range was between 70 and 85 V.% which may be considered to be high aggregate content in the case of geopolymer concrete. Peng Y. and Unluer C. [55] conducted a study using machine learning techniques in data collected from several publications to study the effect of geopolymer concrete variables on its performance. Their study reported that the content of the fine and coarse aggregate had an insignificant influence on compressive strength. Another trend was also found in the literature in the case of the flash metakaolin-based geopolymer, where the total aggregate content yielded an insignificant effect on geopolymer concrete performance in the range of 71 to 83 Wt.%. This was attributed to the strongly developed ITZ [56]. Nevertheless, it was reported that both the total aggregate content and fine aggregate to total aggregate content ratio interacted and played a significant role in determining the performance of geopolymer concrete [57,58]. In these two studies, the total aggregate content varied between 60 and 75 V.% and the fine aggregate ratio varied between 20 and 40 Wt.%. Optimum compressive strength was obtained at a total aggregate content of 70 V.% and a fine aggregate ratio of 35 Wt.%. Similar results were obtained by Joseph and Mathew [59] where almost similar parameters and ranges were considered. The total aggregate content was also reported to affect the geopolymer concrete slump. The higher the aggregate content, the lower the slump value. A zero-slump value was reported for an aggregate content of 80% [60]. The results showed that even with high aggregate content, geopolymer concrete can provide good workability if the binder proportions are controlled. According to Raphaëlle and Martin [56], the higher aggregate content will reduce the total porosity of geopolymer concrete. Their results showed that the total porosity dropped by about 9% as the aggregate content increased from 72% to 83%. Interestingly, such a high aggregate content is expected to increase the total porosity.

The coarse aggregate size was reported to provide a slight strength increment as it increased in the range from 4.75 to 18.75 mm. Beyond this range, a remarkable reduction occurred [61]. In contrast, it was reported that a sharp strength reduction occurred as the mean aggregate size increased from 7.5 to 18 mm in the case of metakaolin-based geopolymer concrete [62]. This can be attributed to the ambient curing that was applied. Ambient curing conditions are known to produce a weak geopolymer binder in the case of metakaolin-based geopolymers [12]. This will enlarge the difference between the elasticity modulus of the binder and the aggregate; hence, strength will be reduced. The aggregate size is also found to be an influencing parameter on the spalling of geopolymer concrete subjected to elevated temperature [63]. In this study, the aggregate size was the only investigated parameter. Three size ranges of coarse aggregate, 2.36–4.75, 4.75–10, and 10–14 mm, were used to produce different geopolymer concrete mixtures. The mixtures' compressive strength was in the range of 44.1–72.4 MPa. The highest strength was obtained for the mixture with the largest size range. The specimens of the mixture with the largest aggregate size did not show explosive spalling at elevated temperatures as compared to mixtures with medium and small aggregate sizes. This was attributed to the reduction in pore pressure due to the increase in the length of the fracture zone and microcracking for larger aggregate particles.

The effect of coarse aggregate size in the range of 5–20 mm on the bond strength between CFRP sheets and geopolymer concrete based on Metakaolin was also investigated. The results revealed that the failure load was reduced by about 15% as the maximum aggregate size increased to 20 mm, while the effective bond length was increased by more

than 40%. It was suggested that the aggregate size should be included in the equations while predicting the bond strength and load capacity [62]. A comprehensive review of the mix design of geopolymer concrete reported that the required volume of coarse aggregate increases as the maximum coarse aggregate size increases and reduces as the fineness modulus of fine aggregate increases [64]. According to Osuji and Inerhunwa [65], the optimum bulk density of different types of aggregate blends can be achieved when the coarse aggregate content is in the range of 50–60 V.% for both rodded and loose aggregate conditions. A higher value for the rodded condition was achieved. This study has only considered the aggregate packing properties and no test was conducted on concrete mixtures.

In summary, the aggregate in the case of geopolymer concrete may provide different behavior from that known for cement concrete. Geopolymer concrete has different reaction mechanisms and different rheological behavior. In the available literature, it was difficult to find an integrated study that was devoted to investigating the aggregate influencing parameters. Additionally, contradictory behavior is reported in the literature. A thorough understanding of the aggregate role is required to develop a clear mixture relationship.

3. Experimental Program

3.1. Materials

Geopolymer concrete mixes were prepared using fly ash (class-F) as the aluminosilicate source material and a mixture of sodium silicate and sodium hydroxide solutions for the alkaline activator choice. The fly ash was obtained from Manjung electric power plant in Perak, Malaysia, and its composition was determined using XRF analysis as given in Table 1. The major crystalline ingredients of fly ash, as obtained from the XRD analysis, were α -quartz, mullite, magnetite, and hematite. The amorphous content was about 56% which indicates the reactivity of this fly ash and its ability to undergo geopolymerization upon activation. The Si/Al ratio and apparent specific gravity of fly ash were 2.08 and 1.91, respectively. A source material with a low Si/Al ratio < 3 is recommended for geopolymer concrete manufacturing [66]. Curing at an elevated temperature (< 100 °C) is usually needed for low-calcium fly-ash-based geopolymers; however, the calcium content (9.9%) of the used fly ash (HCFA) helped to cure the produced concrete at ambient temperature (24 ± 3 °C) [7]. This may provide the produced concrete the privilege to be cast in situ and reduce the environmental impact resulting from curing at elevated temperatures.

Table 1. Chemical composition of the used fly ash (% by mass).

Al ₂ O ₃	Fe ₂ O ₃	SiO ₂	CaO	MgO	SO ₃	P ₂ O ₅	K ₂ O	Na ₂ O	LOI
19.5	17.3	40.6	9.9	1.8	0.7	1.3	2.1	0.29	2.6

The sodium hydroxide and sodium silicate solutions were supplied by Quick Lab, Malaysia. The specific gravity of sodium silicate was 1.55 and it was composed of 29.43% silicon dioxide, 14.26% sodium oxide, and 56.31% water. The sodium hydroxide solution was prepared (one day before mixing, allowing cooling down to room temperature) by dissolving sodium hydroxide pellets of 98% purity in water at a predetermined amount for the required solution concentration.

The used coarse aggregate was a well-shaped angular crushed granite aggregate. The coarse aggregate was sieved and recombined at predetermined ratios to produce 5 blends of the coarse aggregate of 25, 19, 16, 12.5, and 9.5 mm maximum aggregate sizes. These blends conformed to the ASTM C33 [67] requirement for concrete aggregate gradation. The bulk specific gravity (saturated surface dry condition) and water absorption of these blends were 2.63 and 0.63%, 2.64 and 0.63%, 2.66 and 0.65%, 2.67 and 0.66%, and 2.69 and 0.68% for the blends of 25, 19, 16, 12.5, and 9.5 mm maximum aggregate size, respectively. The used fine aggregate was a natural quartz river sand having a maximum particle size of 2.36 mm. The fine aggregate was sieved and recombined at predetermined ratios to

produce 5 blends of sand with 2.4, 2.6, 2.8, 3.0, and 3.2 fineness moduli that also conformed to ASTM C33 [67] requirements. The bulk specific gravity (saturated surface dry condition) and water absorption of these blends were 2.57 and 1.19%, 2.59 and 1.22%, 2.61 and 1.26%, 2.64 and 1.3%, and 2.69 and 1.35% for the blends of fineness moduli of 2.4, 2.6, 2.8, 3.0, and 3.2, respectively.

The fine and coarse aggregates were utilized in a state of saturation where the surface is dry. The evaluation of this condition was based on visual assessment. The coarse aggregate was dampened without leaving any visible film, while the fine aggregate was free-flowing. The objective of using the saturated surface dry condition was to prevent the aggregates from absorbing the alkaline solution or adding excess water to the mixture. This was done to reduce the impact of the aggregate condition on the measured properties.

3.2. Design of Mixtures

The geopolymer concrete mixes were designed using the central composite design. The central composite design is one of the response surface methods (RSMs). It can be effectively used to systematically explore the relationship between parameters (independent variables) and responses (dependent variables) statistically and mathematically and build empirical models [68]. These models can then be used to design mixtures and optimize the required response. Central composite design enables the investigation of the effect of various parameters while minimizing the number of required tests and efforts. In addition, it enables checking whether a second-order effect exists between the investigated parameters.

In this study, most of the parameters related to aggregate were investigated including aggregate volume fractions (AVF), coarse aggregate to the total aggregate ratio (CAR), maximum aggregate size (MAS), and fineness modulus of fine aggregate (FFM). Each parameter was investigated at five levels between the low and high limits as given in Table 2. The low and high levels were specified by considering the possible range that can produce acceptable mixes in terms of workability and consistency (as obtained from a preliminary investigation) while considering the values that are usually used in cement concrete production. The levels for each parameter were determined using circumscribed central composite design. The high and low limits were set to be the extreme points (star points) and then the factorial points were generated. The MAS levels were then adjusted to match the sizes of standard sieves. This type of design enables obtaining a rotatable, spherical, and orthogonal design.

Table 2. Limits of the tested parameters.

Designation	Parameter	Low	High
A	AVF (%)	60	80
B	CAR (%)	45	85
C	MAS (mm)	9.5	25
D	FFM	2.4	3.2

A statistical software called Design-Expert[®] version 13.0.5.0 was used to generate the mixes and analyze the results. Table 3 shows the proportions of the geopolymer concrete mixtures as per the central composite design and the measured responses. The central composite design required 27 mixes to cover the possible combination of the investigated parameters. Three of them (GC3, 22, and 23) were repeated for the central mix. This was necessary to increase the reliability of the predictions throughout the region and particularly close to the center point at which the optimum responses were expected to originate from.

Table 3. Matrix of experimental design and measured responses of geopolymer concrete mixes using central composite design.

Mix Designation	AVF (%)	CAR (%)	MAS (mm)	FFM	Slump (mm)	σ_{28d} (MPa)	Air Content (%)	AVPP (%)
GC1	75	55	12.5	2.6	40	30.5 ± 1.6	9.9	13.3
GC2	60	65	16	2.8	220	48.3 ± 0.7	1.7	10.8
GC3	70	65	16	2.8	145	37.6 ± 0.4	6.7	12.2
GC4	75	75	19	2.6	95	18.7 ± 4.1	8.6	17.1
GC5	65	55	12.5	2.6	140	50.1 ± 0.8	4.2	10.3
GC6	75	55	19	3	75	19.6 ± 3.7	8.7	16.5
GC7	75	55	19	2.6	50	23.9 ± 2.4	9.2	15.4
GC8	70	65	9.5	2.8	110	55.6 ± 0.6	7.2	9.6
GC9	80	65	16	2.8	10	16.9 ± 3.7	9.8	19.2
GC10	70	85	16	2.8	175	21.2 ± 3.3	7	15.4
GC11	65	75	12.5	3	180	42.1 ± 3.2	2.2	12.1
GC12	65	55	19	3	185	39.6 ± 2.6	3.4	11.7
GC13	65	75	19	3	200	35.3 ± 3.2	1.5	11.1
GC14	65	75	12.5	2.6	155	46.8 ± 2.9	2.6	11.1
GC15	75	75	12.5	2.6	70	23.4 ± 3.8	9	15.6
GC16	65	75	19	2.6	170	40.2 ± 3.9	1.9	11.9
GC17	75	75	19	3	110	15.5 ± 4.2	7.6	18.5
GC18	65	55	19	2.6	165	44.7 ± 1.1	3	11.1
GC19	70	65	16	2.4	33	22.8 ± 2.7	7.1	15.9
GC20	65	55	12.5	3	155	45.2 ± 0.9	3.8	11.4
GC21	75	75	12.5	3	90	20.8 ± 3.9	8.1	17.0
GC22	70	65	16	2.8	140	37.9 ± 1.0	6.8	11.5
GC23	70	65	16	2.8	145	37.5 ± 1.3	6.7	12.8
GC24	70	65	25	2.8	155	29.9 ± 2.3	6.4	14.2
GC25	75	55	12.5	3	60	24.8 ± 2.2	8.5	15.1
GC26	70	45	16	2.8	110	27.1 ± 2.4	8.4	14.3
GC27	70	65	16	3.2	160	25.2 ± 2.4	6.3	13.1

The other influencing parameters that control the geopolymer paste properties, including the concentration of sodium hydroxide solution, sodium silicate to total alkaline solution ratio, and alkaline solution to fly ash ratio, have been investigated in previous studies [10,11,69] and were fixed in this study at their optimum values of 10 M, 0.7, and 0.45, respectively. The geopolymer paste produced using these ratios provided a compressive strength of 72.8 ± 0.9 MPa and an initial setting time of 105 min. The ingredients of the mixtures were determined using the absolute volume method [70].

3.3. Preparation and Testing of Specimens

Geopolymer concrete mixtures were prepared and cast in steel molds following the procedures of conventional concrete mixing as specified by ASTM C 192 [71]. All of the dry components were dry-mixed and then the alkaline solution was added and wet-mixed until a consistent mixture was observed. The concrete was then cast into molds and consolidated using a vibrating table. The specimens were stored at controlled temperature and humidity in the range of 24 ± 2 °C and $80 \pm 5\%$, respectively, until the day of testing. For each mix, eight cubes were cast and at least three cubes were tested for compressive strength (i.e., so that the standard deviation for the highest measured value did not exceed 3 MPa and 0.7 MPa for the lowest value; otherwise, the result was excluded); another three were tested for AVPP. The total number of tested specimens was 216.

The compressive strength test was conducted following the EN 12390-3 [72] standards using 150 mm cubes. A compression machine of 3000 kN capacity equipped with a digital data logger was set at a loading rate of $0.2 \text{ N}/(\text{mm}^2 \cdot \text{s})$ and used to conduct the test. The consistency of freshly mixed concrete was evaluated using the slump cone test following ASTM C143 [73] standards. The air content of fresh mixes was measured via the pressure method following ASTM C231 [74] standards. The apparent volume of permeable pores

(AVPPs) was determined following ASTM C642 [75] standards using 100 mm cubes. A scanning electron imaging equipment manufactured by Zeiss, Germany, supra 55 VP, was used in taking and analyzing the scanning electron microscopy (SEM). Figure 1 shows some of the tested specimens and the testing apparatus. The flowchart of the research processes is illustrated in Figure 2.



Figure 1. (a) Concrete specimens, (b) loading machine, (c) slump test, and (d) air content apparatus, respectively.

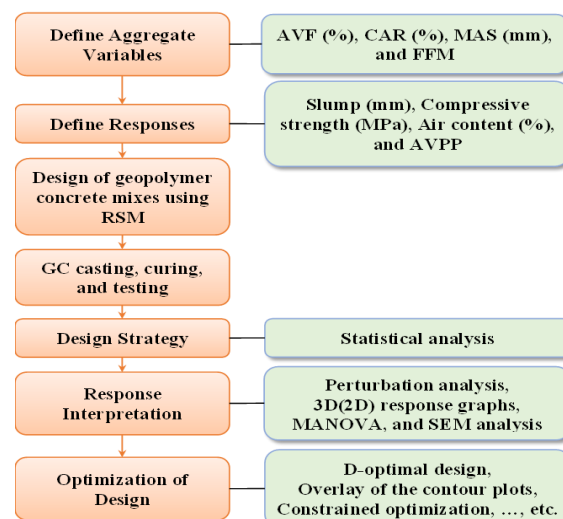


Figure 2. The flowchart of the research processes.

4. Results and Discussion

4.1. Effect of AVFs

Figure 3 shows the effect of AVFs on the compressive strength, slump, and AVPP of geopolymer concrete. The dashed lines represent the confidence intervals (CIs) in which 95% of the expected average values could be found. The compressive strengths of mixtures prepared with higher AVFs were consistently and significantly lower than those of the concretes prepared with lower AVFs. The strength was reduced by more than 70% as the AVFs increased from 60% to 80%. The reduction occurred almost in a linear fashion and started to level off after AVFs decreased to 65%. The reduction in the strength was around 9.5 MPa for each 5% increment in AVFs. The cross-sections for specimens at various AVFs are shown in Figure 4. The variation in the aggregate content compared to the geopolymer paste content at various AVFs can be clearly recognized.

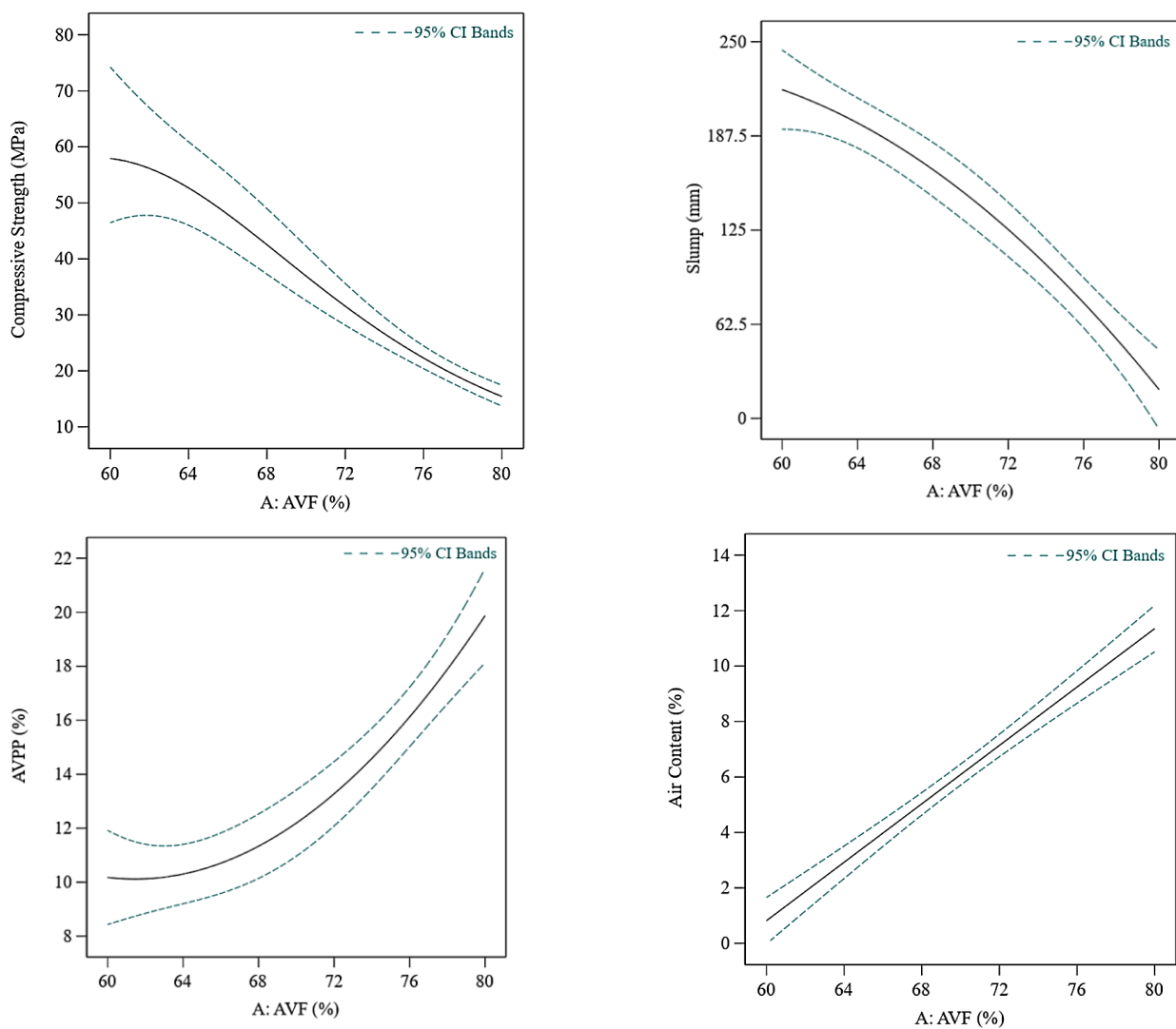


Figure 3. Effect of AVF on compressive strength, slump, AVPP, and air content.

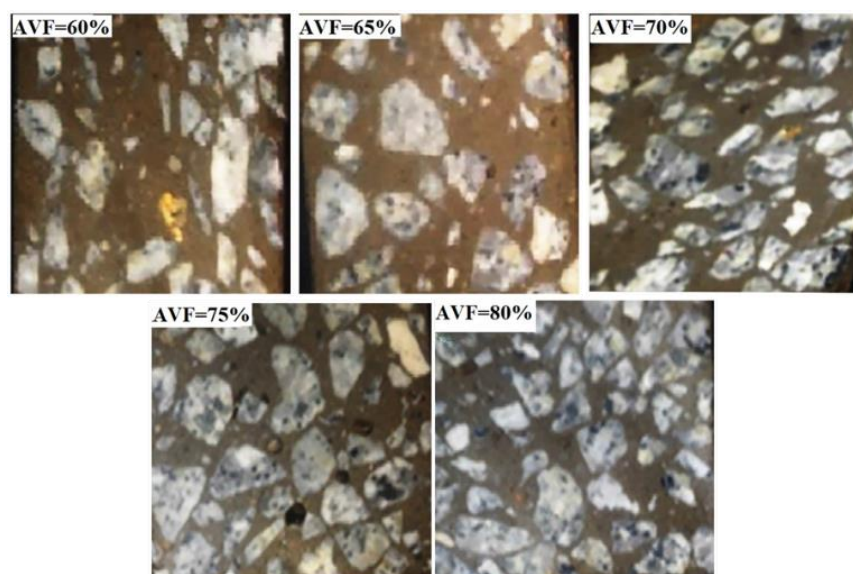


Figure 4. Cross-sections of GC2, GC5, GC13, GC1, and GC9 mixes representing an AVF of 60%, 65%, 70%, 75%, and 80%, respectively.

The effect of AVFs on the slump value was similar to its effect on compressive strength, as can be seen in Figure 3. The curve shows that the slump value was decreasing in an increasing trend as the AVFs increased. The slump value was reduced by more than 90%, whereas the AVFs only varied by 20%. It is worth mentioning that all of the mixes provided a true slump even at the highest AVF. The mixtures provided high coherence of the constituents which can be attributed to the fineness of fly ash particles and the high viscosity of the alkaline solution as compared to water [24]. Moreover, the ease of consolidation and the finishing of mixtures was acceptable even for the mixture with the lowest slump value (about 10 mm). This may refer to the small size of the fly ash particles and their spherical shape which facilitate the sliding and rolling of the larger aggregate particles.

AVFs also affected the AVPP: the AVPP was increasing in an increasing trend as the AVFs increased. The lowest AVPP of about 10% was obtained at an AVF of 60%, while the value increased to about 19% at the highest AVF of 80%. A similar trend was observed by Nikolaos et al. [54], where it was reported that a higher binder-to-aggregate ratio increased the geopolymer concrete strength and durability. Figure 3 shows the effect of AVFs on the air content of the fresh mix. A linear relationship was observed between them, and the air content varied in the range of 1–12% at a constant rate of 2% for each 5% AVF. As compared to ordinary cement concrete, in general, geopolymer concrete provides a higher air content in fresh mixes. This may also be attributed to the higher viscosity of geopolymer concrete mixtures that increased the amount of entrapped air.

Geopolymer concrete is a composite material formed by the combination of the binder phase and the aggregate phase, resulting in the formation of the interfacial transition zone (ITZ) as a new phase. The ITZ phase exhibits higher porosity compared to the binder phase. The increased volume fraction of aggregates (AVFs) in the mixture led to an increase in the volume of the ITZs, bringing their boundaries closer together, which helped bridge the matrix flaws and other discontinuities. This led to an increase in the porosity of the geopolymer concrete, as depicted in Figure 3. The workability of the fresh mixtures also affected the porosity, with lower workability leading to reduced compaction ability. Increasing the amount of aggregate in the mixture required higher amounts of geopolymer paste for coating and lubrication. A higher volume of geopolymer paste, in turn, increased the backing of the aggregate. Figure 3 shows that an increase in AVF from 60% to 80% reduced the slump value by approximately 90%. Conversely, reducing the AVF increased

the amount of geopolymer paste required. The very fine size of the FA particles improved the ITZs properties, while the unreacted FA particles acted as fillers.

Due to its 3D aluminosilicate network and the adhesive properties of the sodium silicate solution, the geopolymer paste itself has superior bonding characteristics and a high strength value (about 73 MPa); this is contrary to the cement paste which usually shows low strength due to volume instability [76]. Furthermore, the difference in the stiffness value of the paste and the aggregate will create a concentration of the stresses at the ITZs. This will reduce the load-carrying capacity of the concrete [77].

Effect of AVFs on the Concrete Microstructure

The BSD-SEM micrographs of geopolymer concrete specimens at varying AVFs are depicted in Figure 5 at 500× magnification level. The geopolymer matrix is a non-uniform aluminosilicate gel that contains some unreacted and partially reacted fly ash particles. These micrographs indicate that a decrease in AVFs leads to a reduction in ITZ width. A lower AVF resulted in higher amounts of fine FA particles and geopolymer gel in the lattice. The size of these particles approaches that of the ITZ, allowing them to fill the ITZs' space and enhance their properties. The micrographs also show that the higher AVFs increased the amount of unreacted fly ash particles, which may also contribute to strength loss. This may be attributed to the lesser amount of the available alkaline solution whereas the aggregate tends to restrain more solution [78,79]. Water plays a significant role in geopolymerization reactions where it is necessary to facilitate alkali transition; less water will hinder the process [12,14]. The wall effect is known in cement concrete where the local water-to-cement ratio at the ITZ can be double what it is within the paste itself [70]. This can also explain the increase in AVPP with the AVFs' increment; the unreacted particles may increase the porosity of the matrix and hence the AVPP may increase too. In addition, the workability was reduced at a higher AVF which may bring the concrete to less of a consolidation state. This is why the air content in the fresh mix also increased. The obtained results confute the hypothesis that claims that the total porosity of geopolymer concrete is only linked to its water content and the addition of aggregate will not create additional porosity [56].

4.2. Effect of CAR

Figure 6 shows the effect of the CAR on the compressive strength, slump, and AVPP of geopolymer concrete. The curve of the CAR and compressive strength was concave downwards with a local maximum representing the optimum CAR. The optimum CAR can be found between 55% and 65%, which corresponds to the highest strength. The difference between the minimum and maximum compressive strength was about 50% as the CAR varied within the investigated range. A similar trend was observed in the case of AVPP. A minimum value of around 12.5% can be obtained between 60% and 65% CARs. A higher or lower CAR will result in a higher AVPP with a greater rate of increase toward the higher CAR. The CAR also affected the slump value, and their variation showed almost a linear trend: the higher the ratio, the greater the slump. Increasing the CAR from 45% to 85% increased the slump value by about 70%. An inverse behavior was found between the CAR and air content. A higher CAR reduced the air content at a constant rate of 0.5% for each 10% CAR.

A lower CAR means introducing more fines to the mix and hence increasing the total surface area of the aggregate. A higher total surface area will require higher amounts of liquid and geopolymer paste to dampen and lubricate the aggregate surface. Therefore, the slump value was reduced as the CAR reduced in the constant alkaline solution to binder ratio and AVFs. The results of strength and AVPP can be explained in terms of concrete compaction. At low CARs, the lower slump values produced stiffer mixes that required greater efforts for compaction. This increased the porosity of the concrete and entrapped more air within the texture resulting in a higher AVPP and lower strength. This can also be observed from the air content of fresh mixes where it was reduced as the CAR

increased. Figure 7 shows the fractured surface of the GC26 mix where the CAR was 45%. The entrapped air bubbles of various sizes can be noticed. As the CAR increased to an optimum value, the workability was enhanced resulting in higher strength and less AVPP. Increasing the CAR further than the optimum value affected the cohesive properties of the mixture. The mix became harsh and relatively difficult to compact. This could explain why the strength started to reduce again and why AVPP increased. In addition, a higher CAR provides less of a surface area for bonding with the geopolymer paste matrix and hence strength will be reduced. It was suggested that the interfacial bonds between the aggregate and geopolymer paste have an optimum surface area at which higher strength stability is achieved. Moreover, the higher fine aggregate content will increase the homogeneity of the mix and enhance the strength accordingly [54].

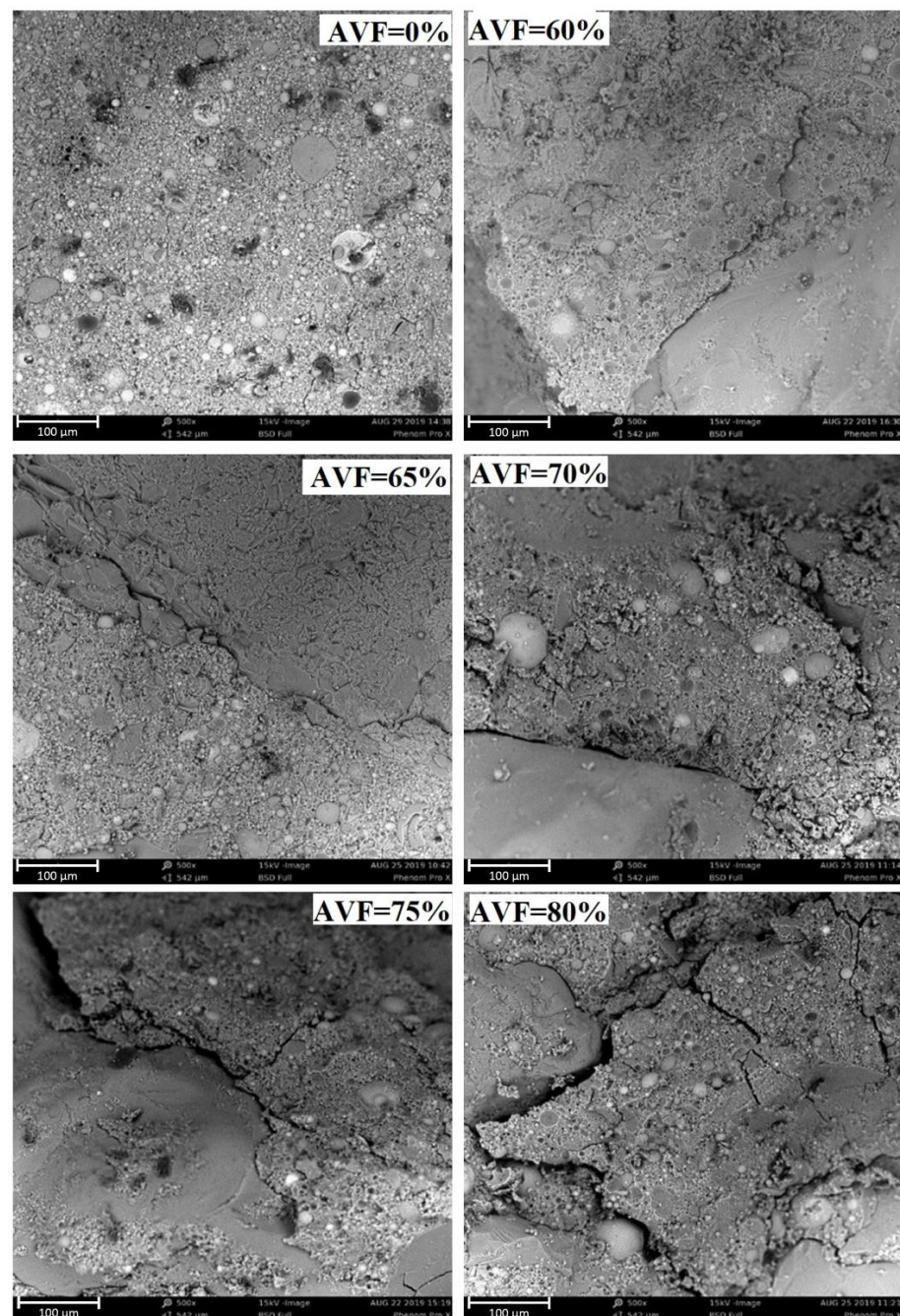


Figure 5. SEM micrographs of the geopolymer paste GC2, GC5, GC13, GC1, and GC9 mixes representing AVFs of 0%, 60%, 65%, 70%, 75%, and 80%, respectively.

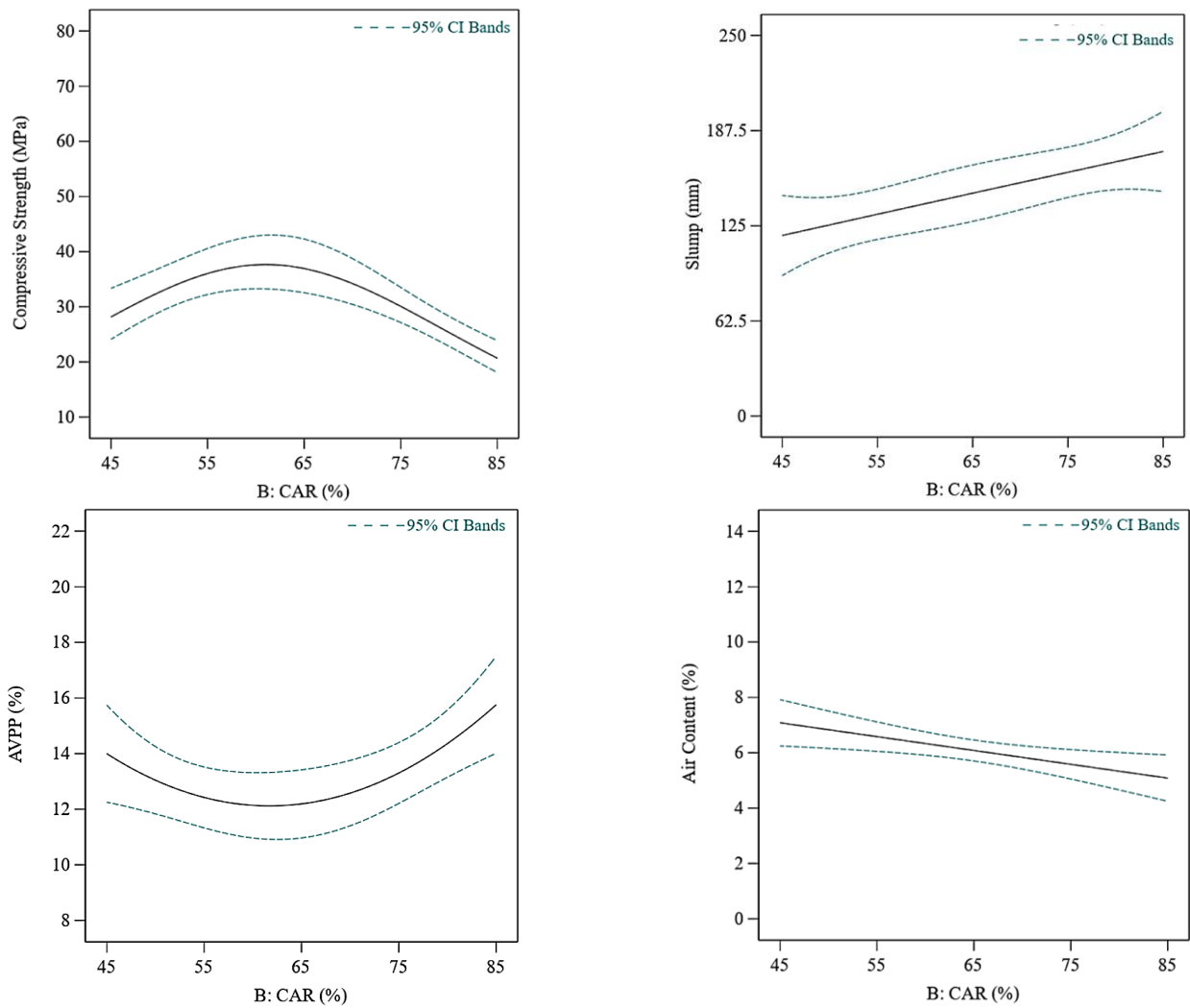


Figure 6. Effect of CAR on compressive strength, slump, AVPP, and air content.

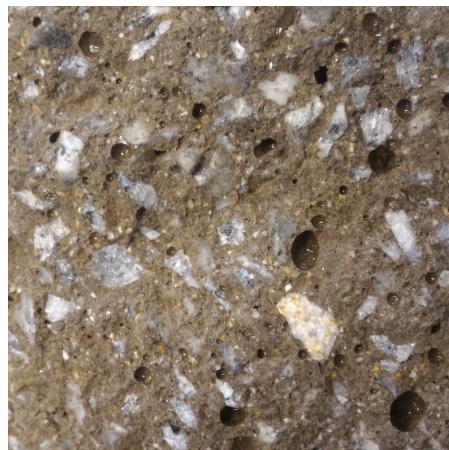


Figure 7. The fractured surface of GC26-mix with CAR = 45%.

4.3. Effect of MAS

Figure 8 shows the effect of MAS on the compressive strength, slump, and AVPP of geopolymer concrete. Increasing the MAS reduced the compressive strength at the whole investigated range at a decreasing rate. Increasing the MAS from 9.5 mm to 25 mm reduced

the strength by more than 20 MPa. In the case of the slump, a reversed trend was observed. The slump increased as the MAS increased for the whole investigated range at a decreasing rate. The measured slump value was reduced by about 48% as MAS increased from the smallest to the largest size. The variation in slump value was higher than the variation in the compressive strength (about 34%) as a response to a change in the MAS. The effect of MAS on the AVPP was similar to its effect on the slump value. The change in the AVPP within the investigated range was around 30%. In the case of the air content of fresh mixes, the air content reduced linearly as the MAS increased; however, the air content changed only by about 1%.

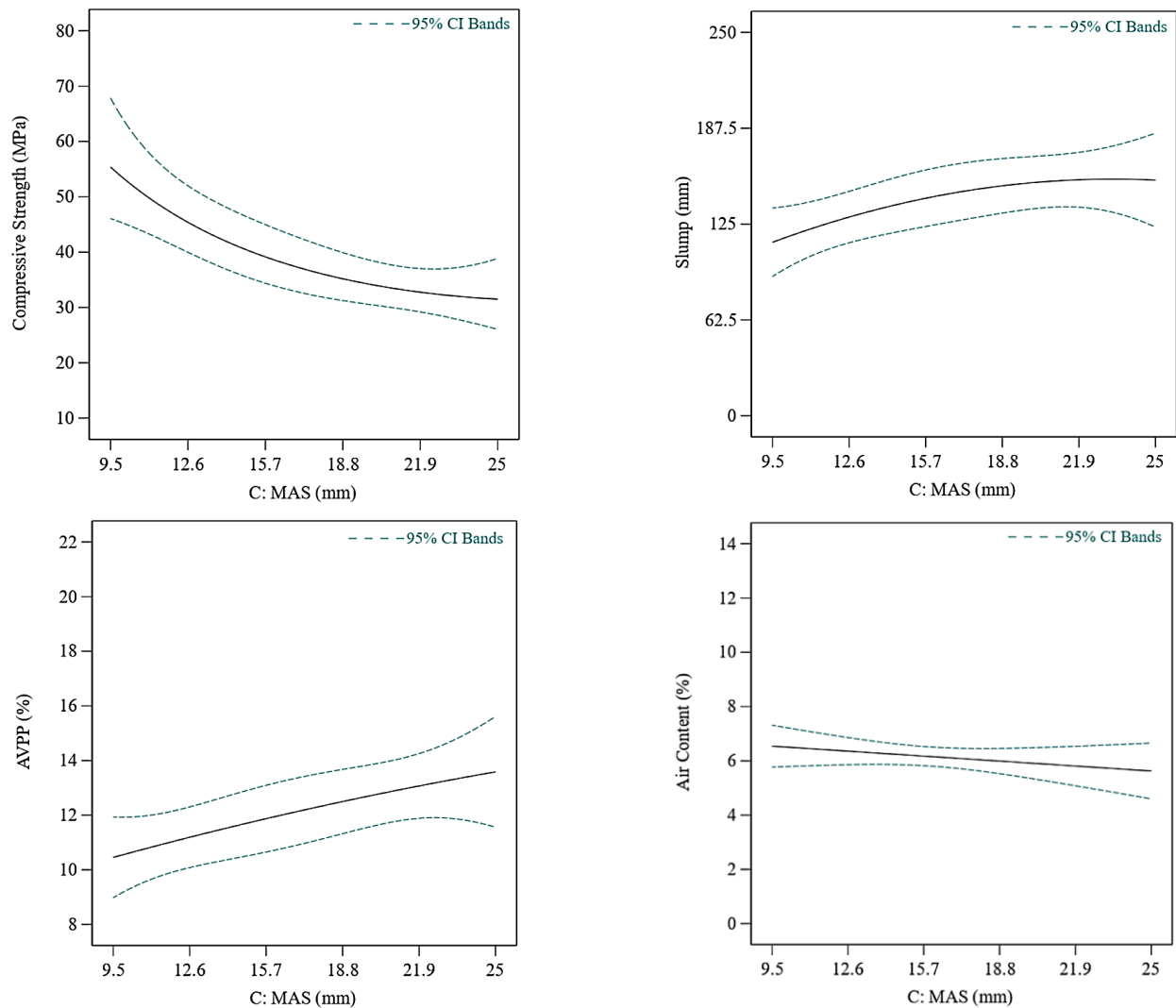


Figure 8. Effect of MAS on compressive strength, slump, AVPP, and air content.

The strength reduction at greater MASs can be clarified for two reasons. The first is that the bond with large aggregate particles tends to be weak as compared with small aggregate particles [61]. This may be attributed to the smaller surface area within a given volume. This behavior is similar to that known in the case of high-strength cement concrete [80]. The second reason is related to the ITZ: the larger aggregate usually generates a wider ITZ [62]. A wider ITZ means introducing weaker zones in which a concentration of stresses occurs and cracks are initiated; later, they can easily interact with the geopolymer paste cracks. As a result of these two reasons, the heterogeneity of the mix will be increased, and there will be more pronounced variations between the aggregate and geopolymer paste in terms of the elasticity modulus, whereby the strength reduces. The MAS effect on slump

value can also be related to the total surface area effect, the same as was explained in the previous section, and to their greater tendency to level off under their own weight. The higher workability is also the reason behind the lower air content of fresh mixes. The effect on AVPP can be referred to as the wall effect. The bigger the aggregate size, the greater the wall effect underneath the particles. The bigger aggregate tends to retain entrapped air bubbles, especially with the high viscosity of the geopolymer paste. In addition, a bigger aggregate will grasp the excess solution while it moves upward and will create voids when it later evaporates.

4.4. Effect of FFM

Figure 9 shows the effect of FFM on the compressive strength, slump, and AVPP of geopolymer concrete. The response of the measured properties to FFM was similar to their response to the CAR. The compressive strength and AVPP provided an optimal value of 38 MPa and 12%, respectively, at almost 2.8 FFM. The compressive strength response showed a more convex shape while the AVPP was less concave. The optimal value was achieved in a wider FFM range that was skewed to the lower FFM value. The maximum variation in compressive strength and AVPP was about 43% and 33%, respectively. Air content showed almost a linear variation with FFM. Its value decreased by 0.25% for each 0.2 FFM increment. The slump value increased in a decreasing trend as the FFM increased. The slump value changed by almost 100 mm as the FFM increased from 2.4 to 3.0. A further increment to 3.2 reduced the slump value a little bit.

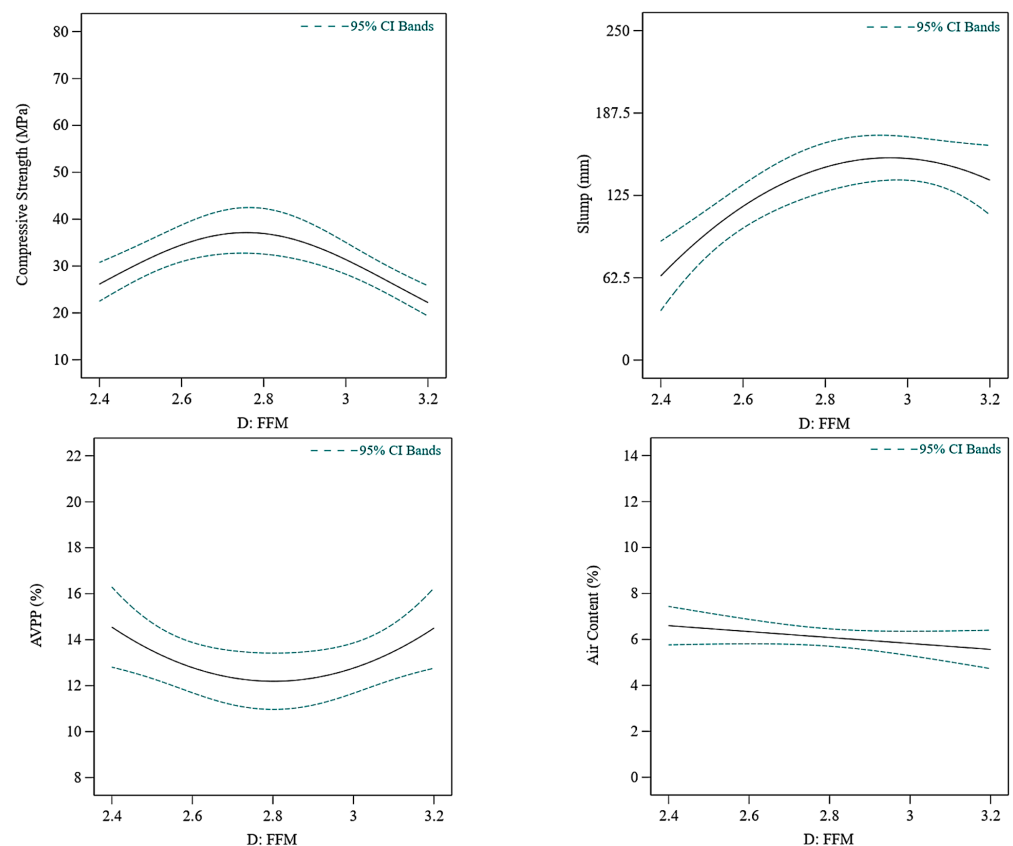


Figure 9. Effect of FFM on compressive strength, slump, AVPP, and air content.

The greater FFM means a coarser grading of the fine aggregate, whereby the reduced surface area increased the obtained slump value. At a fixed AVF, the finer particles in sands require more geopolymer paste to cover and bind them. The shortage of geopolymer paste reduced the mixture's fluidity and strength. Additionally, the finer particles increased the cohesiveness and mixture viscosity and entrapped more air. The optimum content of fines

is required to achieve good binding between the geopolymer paste and aggregate while maintaining workability. To some extent, finer particles will retain a higher amount of alkaline solution which can motivate geopolymerization reactions. Additionally, the divergence in surface area may influence the bleeding and ingress of the alkaline solution.

4.5. SEM-EDX Analysis

To verify whether the aggregate may impact the geopolymerization process or not, an SEM-EDS line scan was conducted on GC19, GC27, GC8, and GC24 samples that represent the extreme point mixtures with FFM = 2.4, FFM = 3.2, MAS = 9.5 mm, and MAS = 25 mm, respectively. Five bands spaced at equal distances of 20 μm were created at the boundary between aggregate and geopolymer paste within the geopolymer paste side, as shown in Figure 10. The EDS spots were taken at three positions within each band. These positions were located on geopolymer binder products and avoided the unreacted fly ash particles. Three samples were analyzed for each mix, and the average value of nine spots (three spots for each band from three samples for each mix) was determined. The results are summarized in Table 4. The table gives only the element with the highest peaks which appeared from the EDS spectra.

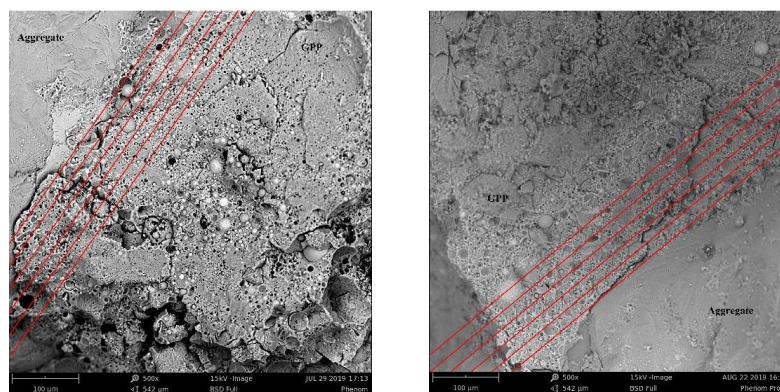


Figure 10. Samples of bands for SEM-EDS analysis.

Table 4. Element concentrations (% \pm STDV *) via SEM-EDS analysis.

Mix	Element	Distance (μm)				
		20	40	60	80	100
GC8	Si	36.7 \pm 4.1	35.3 \pm 3.7	34.6 \pm 1.8	33.8 \pm 3.9	34 \pm 1.9
	Al	10.1 \pm 1.9	10 \pm 2.1	9.9 \pm 3.3	10.3 \pm 1.9	9.8 \pm 3.6
	Na	2.4 \pm 0.5	2.3 \pm 0.6	2.1 \pm 0.5	1.9 \pm 0.5	2.1 \pm 0.4
	Ca	5.3 \pm 0.9	5.1 \pm 0.8	5.2 \pm 1.2	4.5 \pm 0.8	5 \pm 0.6
GC24	Si	40.9 \pm 5.1	39.4 \pm 6.1	34.4 \pm 3.7	33.1 \pm 3.7	33.2 \pm 2.4
	Al	10.8 \pm 2.1	10.7 \pm 2	9.9 \pm 1.5	10 \pm 1.8	9.9 \pm 1.3
	Na	3 \pm 0.5	2.9 \pm 0.5	2.3 \pm 0.3	2 \pm 0.5	2.3 \pm 0.4
	Ca	5.9 \pm 1.6	5.7 \pm 1.5	5 \pm 1.5	4.9 \pm 1.4	4.8 \pm 1.3
GC19	Si	37.3 \pm 2.7	36.9 \pm 4.4	32.5 \pm 3.5	33.1 \pm 1.6	33.5 \pm 3.5
	Al	13.6 \pm 2.4	13.3 \pm 2.2	13.1 \pm 1.9	13.2 \pm 1.8	13.4 \pm 1.2
	Na	2.5 \pm 0.5	2.5 \pm 0.2	2.4 \pm 0.4	2.3 \pm 0.3	2.4 \pm 0.2
	Ca	6.9 \pm 1.2	6.8 \pm 1.3	6.5 \pm 1.4	6.4 \pm 0.9	6.2 \pm 0.8
GC27	Si	41.7 \pm 2.2	41.4 \pm 3.2	36.1 \pm 2.8	32.1 \pm 2.1	32.2 \pm 4
	Al	10.1 \pm 1.6	10.1 \pm 1	10.3 \pm 1.3	9.9 \pm 1.6	10.6 \pm 2
	Na	2.4 \pm 0.6	2.3 \pm 0.4	1.9 \pm 0.5	2.1 \pm 0.3	2.1 \pm 0.2
	Ca	5.4 \pm 1.2	5.4 \pm 2.5	5.5 \pm 1.1	5.2 \pm 0.8	5.3 \pm 0.7

* Standard deviation.

Using SEM-EDS elemental analysis, the geopolymerization process could be evaluated. This could be achieved by considering the Al and Ca concentrations, since the fly ash particles are the only source of these elements. Higher concentrations may indicate enhanced geopolymerization. The Si concentration may not provide a clear indication since the alkaline solution is another source for this element. The Na concentration was mainly provided by the alkaline solution whereas the Na concentration within the fly ash particles was very low, as given in Table 1.

Figure 11 shows the elemental analysis of the investigated mixes at 20 μm and 100 μm bands. The figures show that the concentrations of Si and Na were higher closer to the aggregate interface. This was correct for all of the investigated mixes. On the other hand, the concentrations of Al and Ca were almost the same no matter the distance. This may be related to the wall effect of the aggregate. The aggregate retained higher amounts of the alkaline solution at their interface which increased the Na and Si concentrations. This also contributed to the light increase in the concentration of Al and Ca within the 20 μm band. The availability of the solution will enhance the reactions [69]. By considering the results of different mixtures at the 20 μm band, it can be observed that GC24 and GC19 provided higher concentrations of all elements as compared to GC8 and GC27, respectively. GC24 represents the mix with the biggest aggregate size which may retain the highest amount of solution. This effect disappeared away from the aggregate interface, as can be seen from the 100 μm band in the figure. On the other hand, in the case of GC19, the higher concentrations can still be found even within the 100 μm band. This may indicate an enhanced geopolymerization process. The finest aggregate in GC19 increased the total surface area of the mix and more solution was retained within the texture. One could expect that the strength should increase because of the enhanced reactions but the results revealed the opposite. It is expected that the strength increment due to the enhanced reactions may not overcome the strength reduction that occurred due to poor compaction and additional porosity.

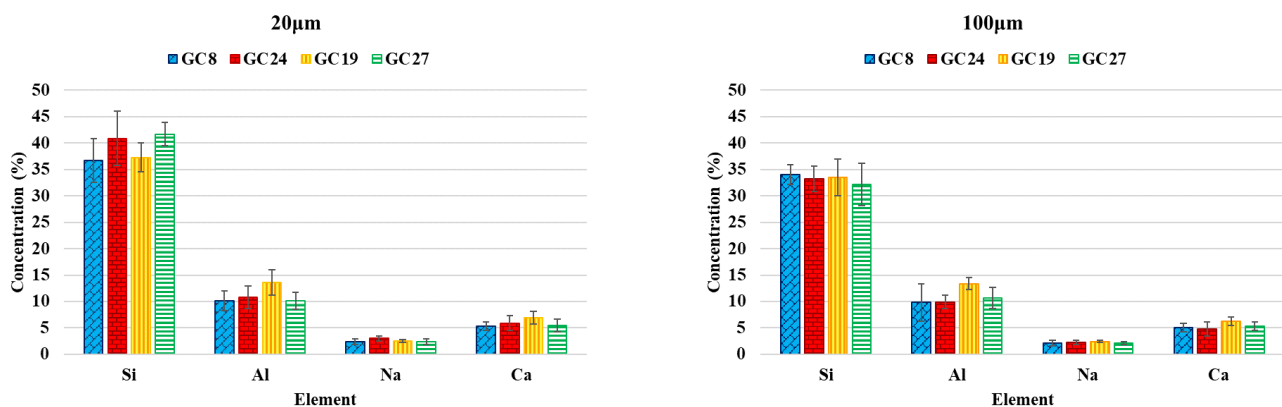


Figure 11. SEM-EDX elemental analysis at 20 μm and 100 μm bands.

To check whether the observed variations can be considered as significant variations, a t-test was conducted with a significance level of 5%. The t-test is a statistical test that can check whether the means of two groups are reliably different from each other. Before conducting the t-test, the normality of the data was checked. The data for each mix were reasonably symmetrically distributed about the mean and the mean was close to the median. The concentrations for all of the mixes showed lower dispersion at the farthest band from the aggregate interface. Within the 20 μm band, the pair GC8–GC24 showed significant variation only for the Na content, while the pair GC19–GC27 showed significant variations in all elements. Between the 20 μm and 100 μm bands, the variations in GC8 were insignificant for all of the elements; in GC24, significant variations were found in Si and Na content; in GC19, significant variations were found in Si content; and in GC27,

significant variations were found in Si content. According to the results, the aggregate may affect the geopolymerization reactions, especially their FFM.

4.6. Statistical Analysis and Response Surfaces

The nonlinear variations between geopolymer concrete constituents (if they existed) can be evaluated using the response surfaces methodology (RSM). RSM provides a statistical and graphical analysis of regression responses. The graphical representation of the measured responses can visually determine the influential variables and their interactions. RSM is usually used for the optimization and development of a response model that represents how the dependent variable (response) will change as a function of the independent variables (parameters). In this study, the development of such models will be beyond the study target. An effective and representative model should consider all of the parameters that are related to the measured response. In our case, the parameters should also include the alkaline solution and source material's properties. These constituents cannot be ignored whereas they can significantly affect the properties of geopolymer concrete as indicated by many researchers. In this study, the aim of carrying out such an analysis is to identify the nonlinearity, interactions, significance, and weight of the investigated parameters.

The RSM was conducted using the multi-analysis of variance (MANOVA) test to fit polynomial models. The independent variables were A = AVF, B = CAR, C = MAS, and D = FFM, and the dependent variables were compressive strength, slump, AVPP, and air content. The MANOVA test indicated that a quadratic equation can best fit the compressive strength response with an F-value of 16.22. Such a large F-value indicates the significance of the suggested model; this response has only a 0.01% opportunity of occurrence due to noise. The multicollinearity phenomenon (in which one parameter can be linearly determined from the others) did not affect the results since the values of the variance inflation factor (VIF) of all of the terms were close to 1. There is a high chance of obtaining the same results upon repeating the design points, whereas a small value of 0.0867 was obtained for the mean square of pure error. The MANOVA results of the compressive strength model are summarized in Table 5.

Table 5. MANOVA of the compressive strength model.

Source	Sum of Square	df	Mean Square	F-Value	p-Value	VIF	Coefficient Estimate
Model	3280.82	14	234.34	16.22	<0.0001		
A-AVF	1674.72	1	1674.72	115.95	<0.0001	1.28	−9.467
B-CAR	73.47	1	73.47	5.09	0.0436	1.28	−1.983
C-MAS	304.60	1	304.60	21.09	0.0006	1.13	−4.196
D-FFM	28.40	1	28.40	1.97	0.01862	1.28	−1.233
AB	1.69	1	1.69	0.1170	0.7382	1.00	−0.325
AC	0.8339	1	0.8339	0.0577	0.8142	1.28	0.272
AD	0.9025	1	0.9025	0.0625	0.8068	1.00	0.237
BC	0.0053	1	0.0053	0.0004	0.9850	1.28	−0.022
BD	1.32	1	1.32	0.0916	0.7674	1.00	0.287
CD	0.1506	1	0.1506	0.0104	0.9204	1.28	0.116
A ²	35.63	1	35.63	2.47	0.1422	1.27	−1.303
B ²	244.94	1	244.94	16.96	0.0014	1.27	−3.415
C ²	26.96	1	26.96	1.87	0.1970	1.38	1.085
D ²	250.35	1	250.35	17.33	0.0013	1.27	−3.453
Residual	173.33	12	14.44				
Lack of Fit	173.24	10	17.32	399.78	0.0025		
Pure Error	0.0867	2	0.0433				

All of the investigated parameters provided a significant first-order effect on the compressive strength of geopolymer concrete, whereas their *p*-value was less than 5%. The response surfaces shown in Figure 12 imply that the curvature effect may be found in all of the investigated parameters. However, the MANOVA revealed that only the CAR

and FFM provided a statistically significant curvature effect with a p -value of less than 5%. This indicates the existence of an optimum value for each of them, at which peak responses can be obtained. Likewise, Figure 12 shows that interactions may be found between AVF and the CAR, AVF and FFM, and the CAR and FFM as two-way slopes can be observed in the response figures. Yet, the MANOVA indicated that, statistically, there were no significant interactions between any of the parameters. This means that changing the value of one parameter will not affect the response of the other parameter. The perturbation blot displayed in Figure 12 demonstrates that AVF and MAS had the highest influence on compressive strength, whereas they show a steeper slope as compared to other parameters. The compressive strength was also more sensitive to the CAR than FFM as it showed a greater curvature response. Table 5 provides the coefficient estimate which quantitatively indicates how the response will change per unit change in the indicated parameter. A higher coefficient estimate value indicates a higher relative effect on the response. The most influential parameters were AVF, MAS, CAR, and FFM, respectively.

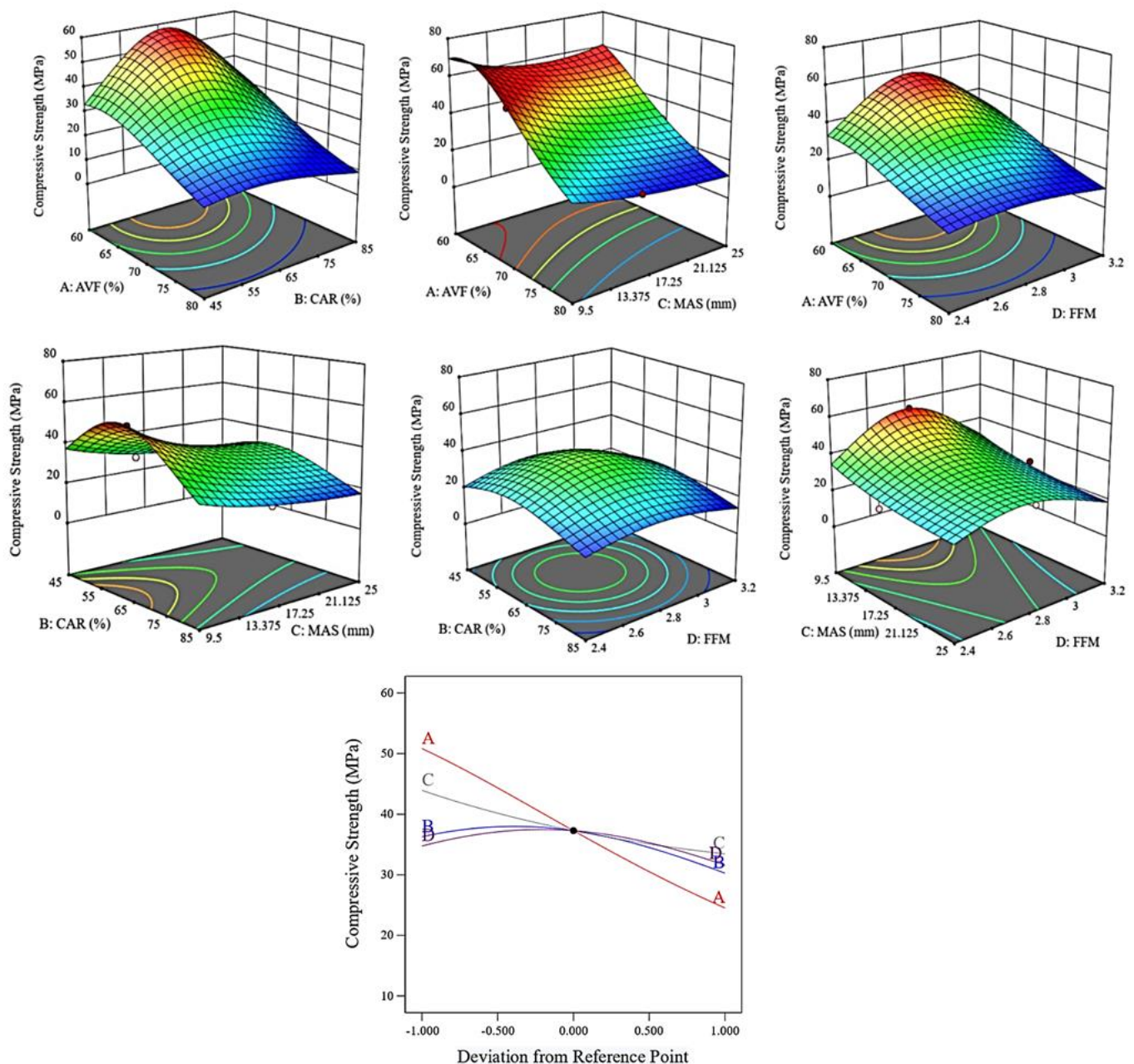


Figure 12. Response surfaces and perturbation plot of the compressive strength model.

A MANOVA test was also conducted on the results of the slump test, AVPP, and air content. The summary of the MANOVA tests is provided in the Appendix A Tables A1–A3 and the response surfaces and perturbation plots are shown in Figures A1–A3. The results of the statistical tests including the F-value, VIF, lack of fit, and mean square of pure error for all of the investigated response models revealed the goodness of the developed models. The best-fit response models of the slump and AVPP were a quadratic model, while the linear model best fits the air content response. At a confidence level of 95%, all of the investigated parameters provided a significant first-order effect on both slump and AVPP responses. However, in the case of air content, only AVF and the CAR revealed significant effects with a p -value of less than 5%. MAS and FFM may consider having a significant effect at an 80% confidence level. No significant interaction effect was observed for any of the investigated parameters, and this was true for all responses. The curvature terms were found to be significant in the case of slump response for FFM, and for AVF, the CAR, and FFM in the case of the AVPP response. The coefficient estimate of the slump model indicated that the most influential parameters were FFM, the CAR, MAS, and AVF, respectively, while in the case of AVPP, the order was AVF, the CAR, MAS, and FFM, respectively. Finally, for the air content response, the order was AVF and then the CAR. The numerical weights of the parameters for each response can be found in Tables A1–A3 by observing the coefficient estimate values.

4.7. Multi-Objective Optimization of Responses

The current study on the fresh and hardened state of geopolymers showed its potential to be produced in a wide range of consistency (10–220 mm) and compressive strength (15–55 MPa) by only controlling the aggregate size and proportions. Additionally, good durability can be guaranteed by controlling the air content and AVPP as they also provided acceptable ranges of 1.5–9.9% air content and 9.6–19.2% AVPP. Therefore, a wide range of applications can be thought of for geopolymer concrete.

The sizing and proportions of aggregate not only affect the properties of geopolymer concrete but also affect its cost as well. Considering the cost of the alkaline solution, the geopolymer paste amount is the major factor governing the geopolymer concrete cost. Accordingly, a good geopolymer concrete mix will be the mix that can achieve the required strength and durability while providing good handling and finishing characteristics and minimizing the amount of the required geopolymer paste. This could be achieved by a good grading and proportioning of aggregate to reduce the voids between the particles and achieve the desirable packing of aggregate. It should be kept in mind that the highest packing of aggregate may provide the highest strength and lowest cost. At the same time, it may reduce workability and durability. The desirability criteria should compromise between them.

Before starting with the optimization of the investigated parameters, it is necessary to understand the relationship (if it existed) between the measured responses (compressive strength, slump, AVPP, and air content) themselves. Interestingly, Figure 13 shows that a specific trend could be found between the investigated responses. The compressive strength revealed a strong correlation with AVPP. A good correlation can also be found between the slump value and air content. It is worth mentioning that the slump reduced as the air content increased. An opposite trend is known for cement concrete: entrained air usually increases the workability where the air bubbles work as a lubricant because of their small size.

A multi-objective optimization was carried out to obtain the best combinations of the investigated parameters that can achieve the desired responses. A regression model was established and tested for each of the measured responses as explained in the previous section. These models were then used to obtain an objective function (desirability function (D)) that could reflect the preferred range for each response (d_i). The range was represented by a value between zero (least desired) to one (most desired). The investigated parameters were varied in a simultaneous and independent manner to achieve the requirement of each

response using a geometric means of individual transformed responses. Then, a global desirability function (D) was obtained using the equation $D = (d_1^{r_1} \cdot d_2^{r_2} \cdot \dots \cdot d_n^{r_n})^{1/\sum r_i}$, in which n is the response number and r is the response importance factor scaled from 1 to 5 as least to most important, respectively [25].

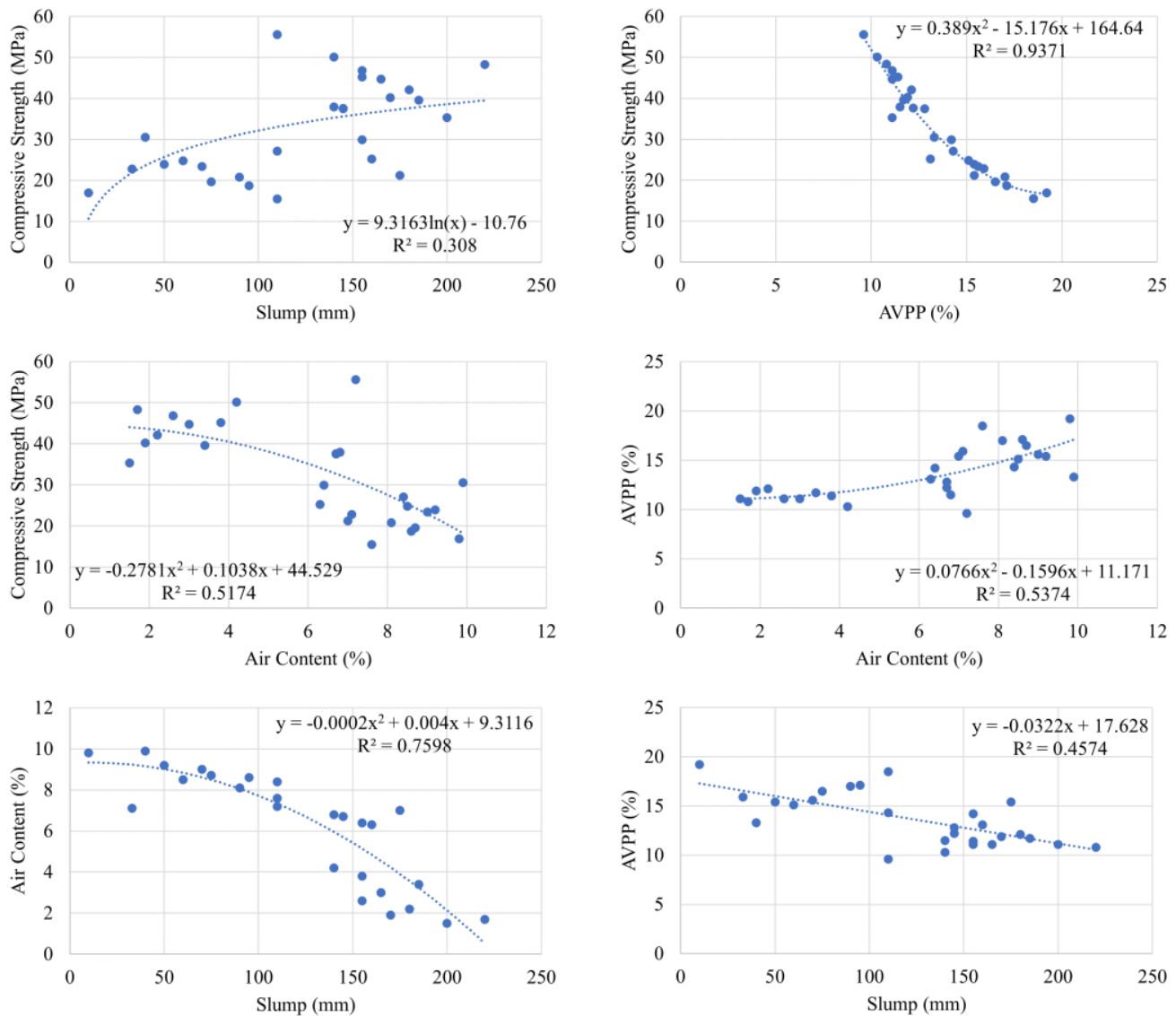


Figure 13. Relationships between the investigated responses.

The target of each response and parameter should be specified as it can be minimized, maximized, hit a specific target, or fall within a specified range. The choices of the desired responses that were used in the Design-Expert® software are presented in Table 6. The compressive strength was set to meet the normal strength of the structural concrete range that is required for most construction works. The slump was selected to meet the range required for concrete of medium consistency. Considering the durability and finishing of concrete, the AVPP and air content were selected to be minimized. All of the responses were considered to have an equal importance level of 3. All of the independent variables were set to be within the range except for the AVF which was maximized to reduce the cost of geopolymer concrete. In order to increase the accuracy of optimization, the range considered for these parameters excluded their extreme values. The Design-Expert® software provided many solutions with desirability values in the range of 0.561–0.513. The ramps of the solution with the highest desirability value are shown in Figure 14. The ramps'

view illustrates the desirability for each parameter and each response. The upper and lower values for each parameter and the expected response are shown. The red points represent the optimal value of each parameter while the blue points represent the prediction values of the optimal response. The range of independent variables that satisfy the optimized solutions was as follows: AVF = 69.9–72%, MAS = 12.5–16 mm, FMM = 2.6–2.7, and CAR = 56.2–74.5%. Proportioning the aggregate within these ranges can produce concrete of 32–43 MPa strength and slump in the range of 90–100 mm. The minimum air content and AVPP were 6.1% and 11.4%, respectively.

Table 6. Criteria sets for multi-objective optimization.

Parameters/Responses	Goal	Lower Limit	Upper Limit
A: AVF (%)	maximize	65	75
B: CAR (%)	is in range	55	75
C: MAS (mm)	is in range	12.5	19
D: FFM	is in range	2.6	3
Slump (mm)	is in range	50	100
Compressive Strength (MPa)	is in range	25	55
Air Content (%)	minimize	1.5	9.9
AVPP (%)	minimize	9.6	19.2

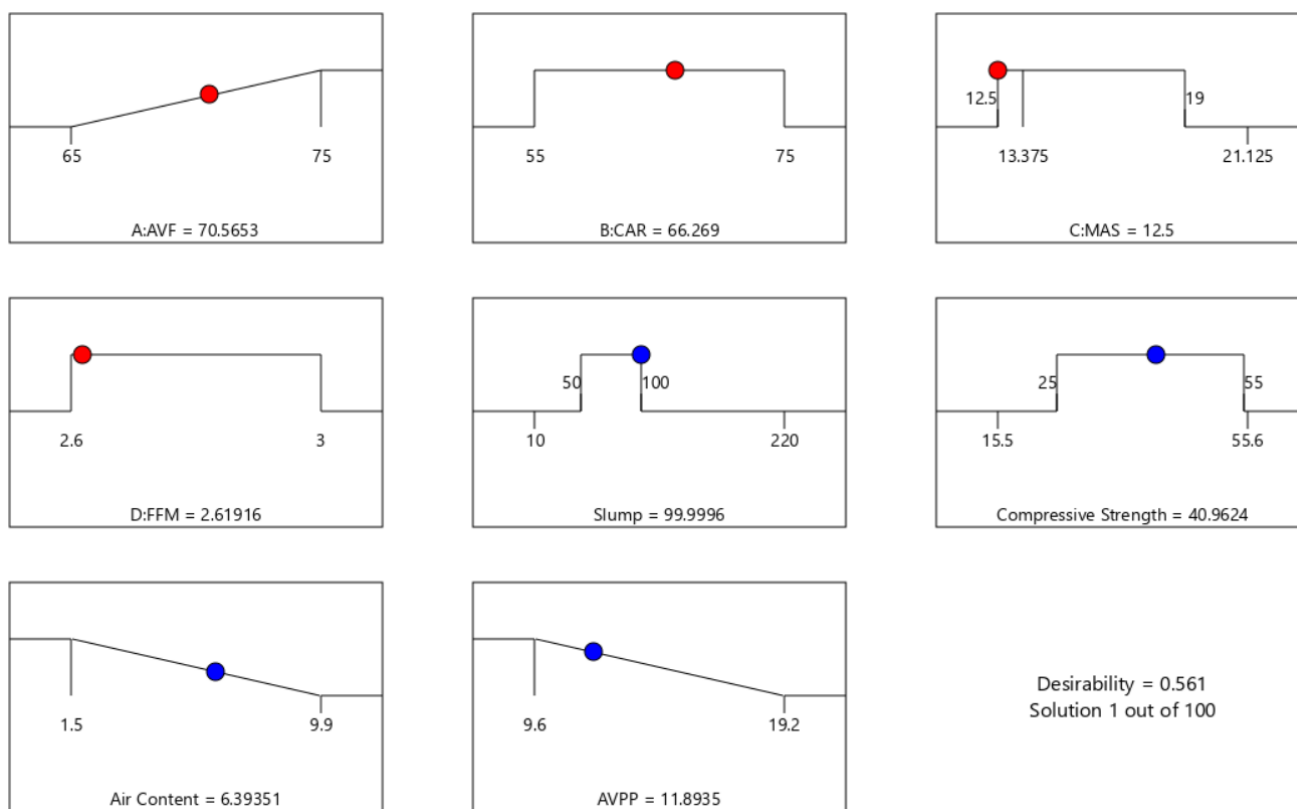


Figure 14. The ramps of the multi-objective optimized responses.

Regression models always need to be validated to examine their accuracy in predicting new observations and to check for the over-fitting possibility. In this study, the optimized results were validated by preparing six new mixes with proportions as presented in Table 7. Two of them were selected out of the optimized solutions based on the solution with the highest and lowest desirability value designated as V1 and V2, respectively. The selection of the remaining four mixes considered the inclusion of different grades of geopolymer concrete compressive strength and new aggregate proportions that differ from the ones

used in the development of the models. This was achieved using the desirability function with a specified target of compressive strength of 20, 30, 40, and 50 MPa. The experimental and predicted results and the average of the absolute prediction errors are given in Table 8. The experimental and predicted results were in acceptable agreement. The prediction error was less than 10%. All of the experimental values were within the 95% high and low prediction intervals. It was noticed that the predictions for all of the responses were more accurate toward the higher compressive strength. No specific error trends can be found, as the models tend to randomly overestimate or underestimate the expected responses.

Table 7. Mix proportions of the validation mixes.

Mix Designation	AVF (%)	CAR (%)	MAS (mm)	FFM
V1	70.6	66.3	12.5	2.7
V2	72.3	58.6	12.5	2.9
V3	70	74.9	25	3
V4	66	74	25	2.7
V5	66	68	19	2.6
V6	68	57	12.5	2.8

Table 8. Experimental and predicted results of the validation mixes.

Slump (mm)			σ_{28d} (MPa)			Air Content (%)			AVPP (%)		
Exp.	Pred.	%Error	Exp.	Pred.	%Error	Exp.	Pred.	%Error	Exp.	Pred.	%Error
110	112.9	−2.6	42.5	43	−1.2	6.6	6.4	3	11.9	11.6	2.5
95	102.1	−7.5	35	37	−5.7	8.5	7.9	7.1	13.4	12.5	6.7
170	185.7	−9.2	19.3	21	−8.8	5.2	5.7	−9.6	17	15.6	8.2
190	201.4	−6	31.6	30.7	2.8	3.4	3.6	−5.9	12.8	13.5	−5.5
165	158.8	3.8	39.2	40.1	−2.3	4	3.9	2.5	11.2	11.8	−5.4
140	136.3	2.6	51.1	50.3	1.6	5.4	5.5	−1.9	10.7	10.4	2.8

Based on the optimization results, the following contour graphs (Figure 15) may provide an effective tool that can be used as a guide in establishing the aggregate proportions for the first trial of geopolymer concrete mixtures in terms of their compressive strength and slump. A further adjustment may be necessary to consider the other mix-design variables.

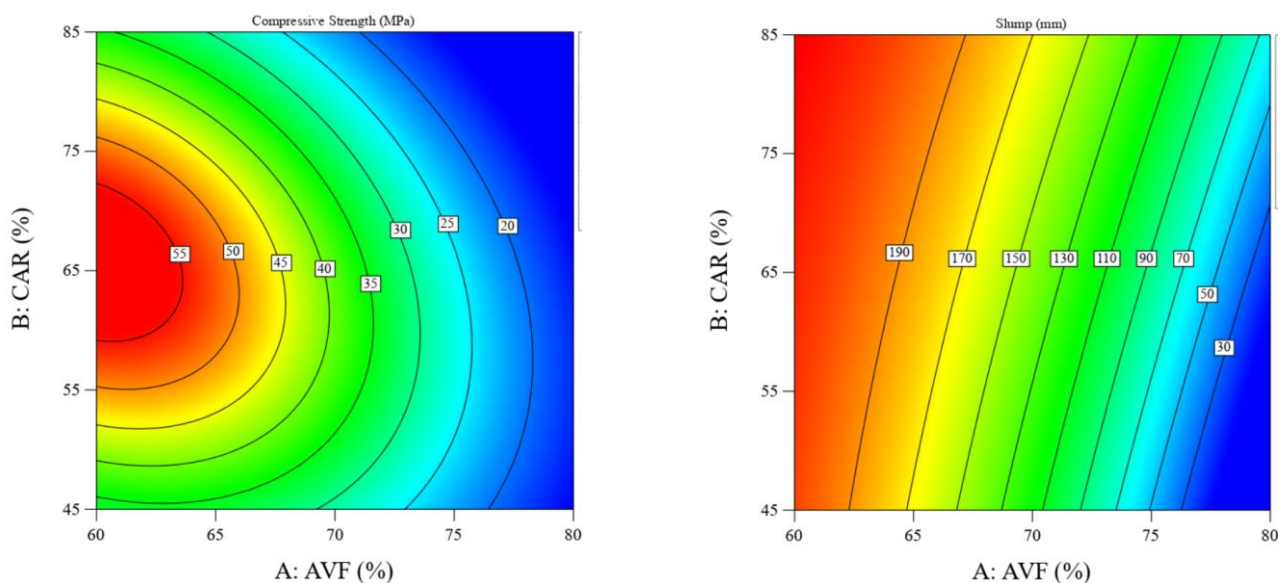


Figure 15. Contour graphs of compressive strength and slump at MAS = 16 mm and FFM = 2.8.

5. Conclusions

A systematic experimental study was undertaken to investigate the effect of aggregate grading and proportions on the fresh and hardened properties of geopolymer concrete. Several conclusions were presented through the discussion, and the following findings can be highlighted:

- The statistical analysis indicated that the investigated aggregate parameters do have a significant effect on the compressive strength, slump, AVPP, and air content of geopolymer concrete. A wide range of consistencies and compressive strengths can be achieved by controlling these parameters.
- Considering that the geopolymer paste phase nominally provides the same strength, the strength variations in mixtures having different aggregate parameters can mainly be attributed to the variation in the microstructure and ITZ. Moreover, SEM-EDS analysis revealed statistically significant variations in the elemental concentrations of the produced geopolymer paste for different aggregate mixtures. This means that aggregate can also alter the geopolymerization process.
- The most influential aggregate parameter in terms of compressive strength, AVPP, and air content was the AVF, while the FFM had the least effect. Yet, the FFM was the main parameter affecting the geopolymer concrete slump.
- Within limits, a higher fine content seems to increase the homogeneity of the mix and enhance the strength of geopolymer concrete. This is dissimilar to the behavior known for cement concrete, where a higher AVF and larger MAS usually increase the strength of cement concrete. This could be attributed to the strong geopolymer binder and its different rheological properties.
- Unlike the current thinking, in the case of geopolymer concrete, aggregate had a significant effect on the air content of freshly mixed concrete. Additionally, the air content is much higher than that in cement concrete. A possible reason for this is the higher viscosity of the geopolymer concrete mixtures. An inverse relationship was found between the slump and air content, which is opposite to the trend known for cement concrete, where entrained air boosts workability as the small size of the air bubbles brings them to work as a lubricant.
- Aggregate plays a significant role in the AVPP of geopolymer concrete, which confutes the hypothesis that the total porosity of geopolymer concrete is only linked to its water content and that the addition of aggregate will not create additional porosity.
- RSM can provide a time-efficient and reliable statistical method for the design of geopolymer concrete with a counterbalance among the design parameters. Yet, the development of statistical models will need a large database beforehand.

There are a few limitations to this study. First, the study considers the aggregate parameters only without considering the binder's influencing parameters that were fixed in this study. An interaction may exist between the binder and aggregate parameters. The investigation of all of the parameters together will require a huge number of specimens, time, and cost. Second, the aggregate type itself may influence their response depending on their source.

Funding: This research received no external funding.

Data Availability Statement: The data presented in this study are available on request from the corresponding author.

Acknowledgments: The author acknowledges the concrete laboratory at Universiti Teknologi PETRONAS, Perak, Malaysia, for providing technical and scientific assistance throughout the experimental works.

Conflicts of Interest: The author declares no conflict of interest.

Appendix A

Table A1. MANOVA of slump model.

Source	Sum of Square	df	Mean Square	F-Value	p-Value	VIF	Coefficient Estimate
Model	76,848.42	14	5489.17	23.71	<0.0001		
A-AVF	46,276.88	1	46,276.88	199.93	<0.0001	1.28	146.41
B-CAR	3554.17	1	3554.17	15.35	0.0020	1.28	−49.77
C-MAS	1778.27	1	1778.27	7.68	0.0169	1.13	13.79
D-FFM	6171.71	1	6171.71	26.66	0.0002	1.28	10.14
AB	400.00	1	400.00	1.73	0.2132	1.00	18.17
AC	30.33	1	30.33	0.1310	0.7237	1.28	5
AD	6.25	1	6.25	0.0270	0.8722	1.00	−1.64
BC	0.1476	1	0.1476	0.0006	0.9803	1.28	−0.63
BD	6.25	1	6.25	0.0270	0.8722	1.00	0.11
CD	21.73	1	21.73	0.0939	0.7645	1.28	0.63
A ²	1006.66	1	1006.66	4.35	0.0591	1.27	1.39
B ²	0.0486	1	0.0486	0.0002	0.9887	1.27	−6.92
C ²	242.16	1	242.16	1.05	0.3266	1.38	−0.05
D ²	2800.91	1	2800.91	12.10	0.0046	1.27	−3.25
Residual	2777.65	12	231.47				
Lack of Fit	2760.99	10	276.10	33.13	0.0296		
Pure Error	16.67	2	8.33				

Table A2. MANOVA of the AVPP model.

Source	Sum of Square	df	Mean Square	F-Value	p-Value	VIF	Coefficient Estimate
Model	164.65	14	11.76	27.27	<0.0001		
A-AVF	98.20	1	98.20	227.68	<0.0001	1.28	12.3
B-CAR	6.43	1	6.43	14.91	0.0023	1.28	2.29
C-MAS	11.48	1	11.48	26.61	0.0002	1.13	0.59
D-FFM	1.80	1	1.80	4.16	0.0064	1.28	0.81
AB	1.77	1	1.77	4.10	0.0657	1	0.31
AC	1.30	1	1.30	3.01	0.1081	1.28	0.33
AD	0.5852	1	0.5852	1.36	0.2667	1	0.34
BC	0.1038	1	0.1038	0.2406	0.6326	1.28	0.19
BD	0.0064	1	0.0064	0.0148	0.9051	1	0.1
CD	0.0561	1	0.0561	0.1300	0.7247	1.28	−0.02
A ²	5.91	1	5.91	13.70	0.0030	1.27	0.07
B ²	11.40	1	11.40	26.43	0.0002	1.27	0.53
C ²	0.5376	1	0.5376	1.25	0.2861	1.38	0.74
D ²	11.25	1	11.25	26.07	0.0003	1.27	−0.15
Residual	5.18	12	0.4313				
Lack of Fit	5.17	10	0.5173	397.92	0.0025		
Pure Error	0.0026	2	0.0013				

Table A3. MANOVA of air content model.

Source	Sum of Square	df	Mean Square	F-Value	p-Value	VIF	Coefficient Estimate
Model	175.05	4	43.76	56.32	<0.0001		
A-AVF	166.43	1	166.43	214.18	<0.0001	1	2.63
B-CAR	6.00	1	6.00	7.72	0.0109	1	-0.5
C-MAS	1.02	1	1.02	1.32	0.1637	1	-0.23
D-FFM	1.60	1	1.60	2.06	0.1652	1	-0.26
Residual	17.09	22	0.7770				
Lack of Fit	17.09	20	0.8544	256.32	0.0039		
Pure Error	0.0067	2	0.0033				
Cor Total	192.15	26					

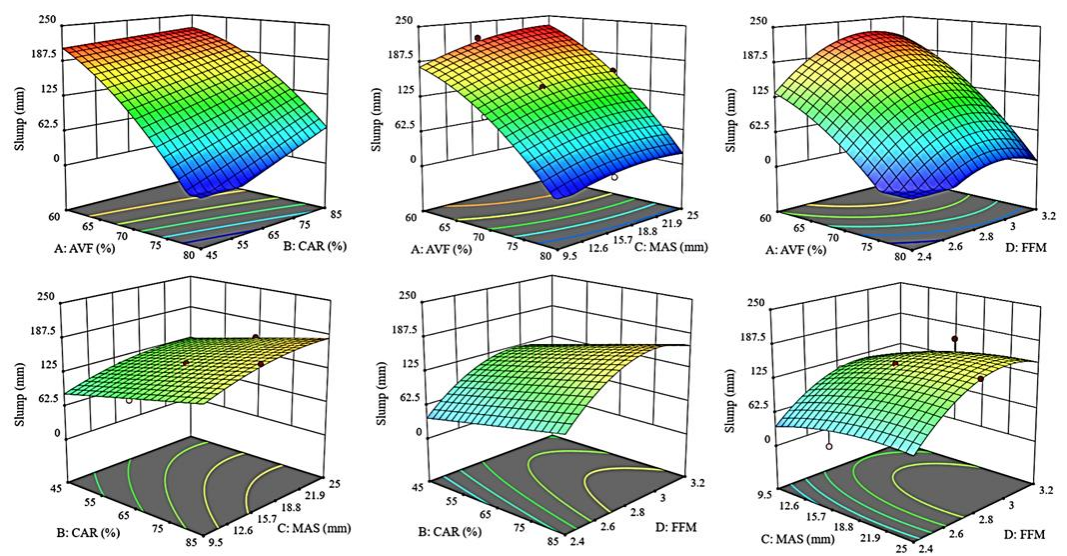


Figure A1. Response surface of slump model.

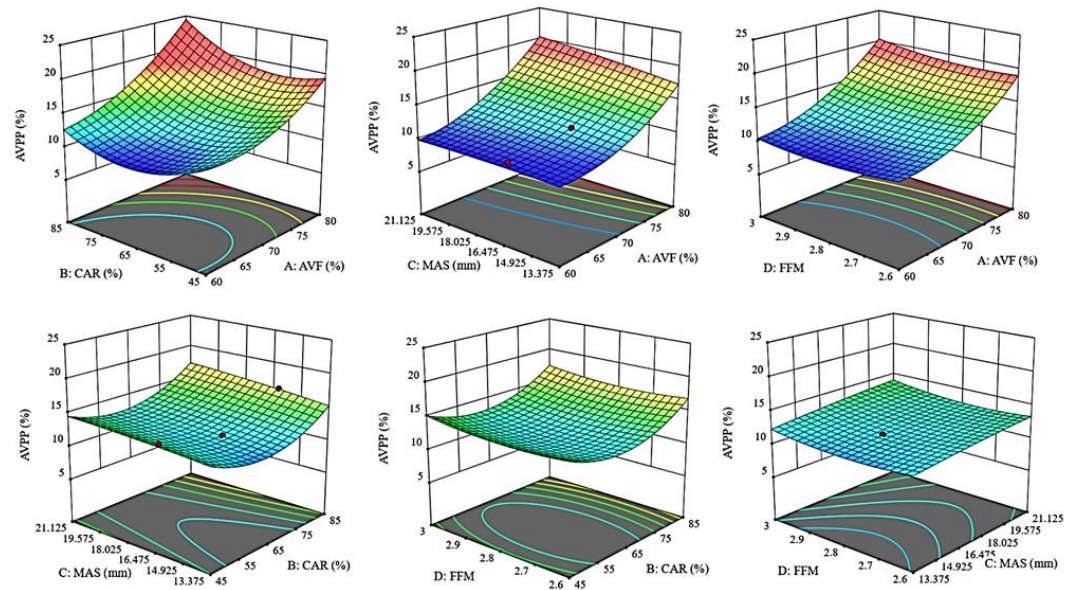


Figure A2. Response surface of the AVPP model.

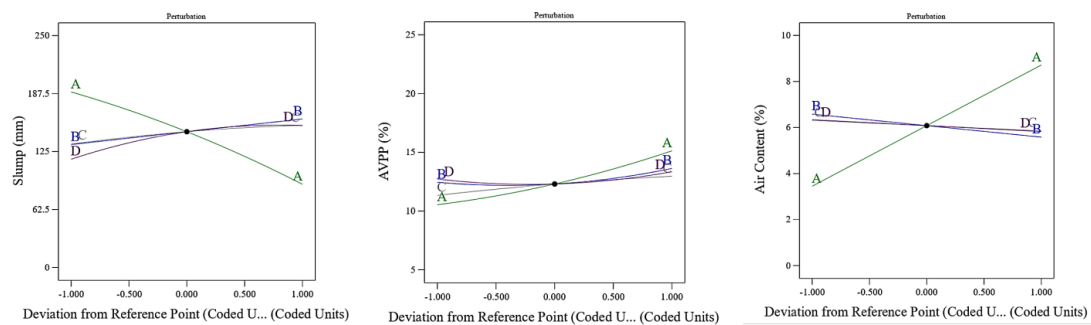


Figure A3. Perturbation plot of the slump, AVPP, and air content: A = AVF, B = CAR, C = MAS, and D = FFM.

References

1. Programme, U.N.E. Sustainability. Available online: <https://unesdoc.unesco.org/ark:/48223/pf0000247444> (accessed on 10 March 2023).
2. World Health Organization. *World Health Statistics 2021: Monitoring Health for the SDGs, Sustainable Development Goals*; World Health Organization: Geneva, Switzerland, 2021. Available online: <https://apps.who.int/iris/handle/10665/342703> (accessed on 10 March 2023).
3. Alaloul, W.S.; Al Salaheen, M.; Malkawi, A.B.; Alzubi, K.; Al-Sabaeei, A.M.; Musarat, M.A. Utilizing of oil shale ash as a construction material: A systematic review. *Constr. Build. Mater.* **2021**, *299*, 123844. [CrossRef]
4. Statista. Global Cement Production 1995–2022. Available online: <https://www.statista.com/statistics/1087115/global-cement-production-volume/#statisticContainer> (accessed on 10 March 2023).
5. Zhang, J.; Li, H.; Xia, B.; Skitmore, M. Impact of environment regulation on the efficiency of regional construction industry: A 3-stage Data Envelopment Analysis (DEA). *J. Clean. Prod.* **2018**, *200*, 770–780. [CrossRef]
6. Zhang, J.; Ouyang, Y.; Ballesteros-Pérez, P.; Li, H.; Philbin, S.P.; Li, Z.; Skitmore, M. Understanding the impact of environmental regulations on green technology innovation efficiency in the construction industry. *Sustain. Cities Soc.* **2021**, *65*, 102647. [CrossRef]
7. Malkawi, A.B.; Al-Mattarneh, H.; Achara, B.E.; Muhammed, B.S.; Nuruddin, M.F. Dielectric properties for characterization of fly ash-based geopolymer binders. *Constr. Build. Mater.* **2018**, *189*, 19–32. [CrossRef]
8. Kai, M.-F.; Dai, J.-G. Understanding geopolymer binder-aggregate interfacial characteristics at molecular level. *Cem. Concr. Res.* **2021**, *149*, 106582. [CrossRef]
9. Nuruddin, M.F.; Malkawi, A.B.; Fauzi, A.; Mohammed, B.S.; Almattarneh, H.M. Geopolymer concrete for structural use: Recent findings and limitations. *IOP Conf. Ser. Mater. Sci. Eng.* **2016**, *133*, 012021. [CrossRef]
10. Fauzi, A.; Nuruddin, M.F.; Malkawi, A.B.; Abdullah, B.; Al, M.M.; Mohammed, B.S. Effect of Alkaline Solution to Fly Ash Ratio on Geopolymer Mortar Properties. *Key Eng. Mater.* **2017**, *733*, 85–88.
11. Malkawi, A.B.; Nuruddin, M.F.; Fauzi, A.; Almattarneh, H.; Mohammed, B.S. Effects of alkaline solution on properties of the HCFA geopolymer mortars. *Procedia Eng.* **2016**, *148*, 710–717. [CrossRef]
12. Nuruddin, M.F.; Malkawi, A.B.; Fauzi, A.; Mohammed, B.S.; Almattarneh, H.M. Evolution of geopolymer binders: A review. *IOP Conf. Ser. Mater. Sci. Eng.* **2016**, *133*, 012052. [CrossRef]
13. Alexander, M.; Mindess, S. *Aggregates in Concrete*; CRC Press: Boca Raton, FL, USA, 2010.
14. Hajimohammadi, A.; Ngo, T.; Kashani, A. Glass waste versus sand as aggregates: The characteristics of the evolving geopolymer binders. *J. Clean. Prod.* **2018**, *193*, 593–603. [CrossRef]
15. Isabella, C.; Lukey, G.C.; Xu, H.; van Deventer, J.S. The effect of aggregate particle size on formation of geopolymeric gel. In *Proceedings of the Advanced Materials for Construction of Bridges, Buildings, and Other Structures III*, Davos, Switzerland, 7–12 September 2003.
16. Wan, Q.; Rao, F.; Song, S.; Cholico-González, D.F.; Ortiz, N.L. Combination formation in the reinforcement of metakaolin geopolymers with quartz sand. *Cem. Concr. Compos.* **2017**, *80*, 115–122. [CrossRef]
17. Keke, S.; Xiaoqin, P.; Shuping, W.; Lu, Z. Design method for the mix proportion of geopolymer concrete based on the paste thickness of coated aggregate. *J. Clean. Prod.* **2019**, *232*, 508–517. [CrossRef]
18. Škvára, F.; Doležal, J.; Svoboda, P.; Kopecký, L.; Pawlasová, S.; Lucuk, M.; Dvořáček, K.; Beksa, M.; Myšková, L.; Šulc, R. Concrete based on fly ash geopolymers. In *Proceedings of the IBAUSIL*, Weimar, Germany, 20–23 September 2006.
19. Lee, W.; Van Deventer, J. The interface between natural siliceous aggregates and geopolymers. *Cem. Concr. Res.* **2004**, *34*, 195–206. [CrossRef]
20. Fang, C.; Xie, J.; Zhang, B.; Yuan, B.; Wang, C. Impact properties of geopolymeric concrete: A state-of-the-art review. *IOP Conf. Ser. Mater. Sci. Eng.* **2018**, *284*, 012012. [CrossRef]
21. Kargari, A.; Eskandari-Naddaf, H.; Kazemi, R. Effect of cement strength class on the generalization of Abrams' law. *Struct. Concr.* **2019**, *20*, 493–505. [CrossRef]
22. 221R-96; Guide for Use of Normal Weight and Heavyweight Aggregates in Concrete. Technical Documents; American Concrete Institute: Farmington Hills, MI, USA, 2001.

23. Tasdemir, M.; Karihaloo, B. Effect of type and volume fraction of aggregate on the fracture properties of concrete. *Mech. Concr. Struct* **2001**, *178*, 123–129.
24. Malkawi, A.B.; Nuruddin, M.F.; Fauzi, A.; Al-Mattarneh, H.; Mohammed, B.S. Effect of plasticizers and water on properties of HCFA geopolymers. *Key Eng. Mater.* **2017**, *733*, 76–79.
25. Ferdosian, I.; Camões, A. Eco-efficient ultra-high performance concrete development by means of response surface methodology. *Cem. Concr. Compos.* **2017**, *84*, 146–156. [[CrossRef](#)]
26. Olivia, M.; Nikraz, H. Properties of fly ash geopolymer concrete designed by Taguchi method. *Mater. Des.* **2012**, *36*, 191–198. [[CrossRef](#)]
27. Fauzi, A.; Nuruddin, M.F.; Malkawi, A.B.; Abdullah, M.M.A.B. Study of fly ash characterization as a cementitious material. *Procedia Eng.* **2016**, *148*, 487–493. [[CrossRef](#)]
28. Kumar, G.; Mishra, S.S. Effect of recycled concrete aggregate on mechanical, physical and durability properties of GGBS–fly ash-based geopolymer concrete. *Innov. Infrastruct. Solut.* **2022**, *7*, 237. [[CrossRef](#)]
29. Malkawi, A.B.; Habib, M.; Aladwan, J.; Alzubi, Y. Engineering properties of fibre reinforced lightweight geopolymer concrete using palm oil biowastes. *Aust. J. Civ. Eng.* **2020**, *18*, 82–92. [[CrossRef](#)]
30. Gunasekera, C.; Law, D.W.; Setunge, S. Effect of geopolymer aggregate on strength and microstructure of concrete. *ACI Mater. J.* **2018**, *115*, 899–908. [[CrossRef](#)]
31. Alanazi, H. Effect of Aggregate Types on the Mechanical Properties of Traditional Concrete and Geopolymer Concrete. *Crystals* **2021**, *11*, 1110. [[CrossRef](#)]
32. B Malkawi, A.; Aladwan, J.; Al-Salaheen, M. Agricultural Palm Oil Wastes for Development of Structural Lightweight Concrete. *Int. J. Civ. Eng. Technol.* **2019**, *10*, 175–183.
33. Sun, K.; Peng, X.; Chu, S.; Wang, S.; Zeng, L.; Ji, G. Utilization of BOF steel slag aggregate in metakaolin-based geopolymer. *Constr. Build. Mater.* **2021**, *300*, 124024. [[CrossRef](#)]
34. Malkawi, A.B.; Habib, M.; Alzubi, Y.; Aladwan, J. Engineering properties of lightweight geopolymer concrete using palm oil clinker aggregate. *Int. J. Geomate* **2020**, *18*, 132–139. [[CrossRef](#)]
35. Eroshkina, N.; Korovkin, M. Influence of Aggregate Type on Properties of Geopolymer Concrete. *IOP Conf. Ser. Mater. Sci. Eng.* **2021**, *1079*, 052058. [[CrossRef](#)]
36. Rashidian-Dezfouli, H.; Rangaraju, P.R. Study on the effect of selected parameters on the alkali-silica reaction of aggregate in ground glass fiber and fly ash-based geopolymer mortars. *Constr. Build. Mater.* **2021**, *271*, 121549. [[CrossRef](#)]
37. Assi, L.N.; Deaver, E.E.; ElBatouny, M.K.; Ziehl, P. Investigation of early compressive strength of fly ash-based geopolymer concrete. *Constr. Build. Mater.* **2016**, *112*, 807–815. [[CrossRef](#)]
38. Ulloa, N.A.; Baykara, H.; Cornejo, M.H.; Rigail, A.; Paredes, C.; Villalba, J.L. Application-oriented mix design optimization and characterization of zeolite-based geopolymer mortars. *Constr. Build. Mater.* **2018**, *174*, 138–149. [[CrossRef](#)]
39. Tahir, M.F.M.; Abdullah, M.M.A.; Hasan, M.R.M.; Zailani, W.W.A. Optimization of Fly Ash Based Geopolymer Mix Design for Rigid Pavement Application. In Proceedings of the 5th International Conference on Green Design and Manufacture (IConGDM), Kota Bandung, Indonesia, 29–30 April 2019.
40. Kupaei, R.H.; Alengaram, U.J.; Bin Jumaat, M.Z.; Nikraz, H. Mix design for fly ash based oil palm shell geopolymer lightweight concrete. *Constr. Build. Mater.* **2013**, *43*, 490–496. [[CrossRef](#)]
41. Abdollahnejad, Z.; Pacheco-Torgal, F.; Felix, T.; Tahrir, W.; Aguiar, J.B. Mix design, properties and cost analysis of fly ash-based geopolymer foam. *Constr. Build. Mater.* **2015**, *80*, 18–30. [[CrossRef](#)]
42. Chu, S.H.; Ye, H.; Huang, L.; Li, L.G. Carbon fiber reinforced geopolymer (FRG) mix design based on liquid film thickness. *Constr. Build. Mater.* **2021**, *269*, 121278. [[CrossRef](#)]
43. Li, X.; Rao, F.; Song, S.; Corona-Arroyo, M.A.; Ortiz-Lara, N.; Aguilar-Reyes, E.A. Effects of aggregates on the mechanical properties and microstructure of geothermal metakaolin-based geopolymers. *Results Phys.* **2018**, *11*, 267–273. [[CrossRef](#)]
44. Arellano-Aguilar, R.; Burciaga-Díaz, O.; Gorokhovskiy, A.; Escalante-García, J.I. Geopolymer mortars based on a low grade metakaolin: Effects of the chemical composition, temperature and aggregate:binder ratio. *Constr. Build. Mater.* **2014**, *50*, 642–648. [[CrossRef](#)]
45. Mermerdaş, K.; Manguri, S.; Nassani, D.E.; Oleiwi, S.M. Effect of aggregate properties on the mechanical and absorption characteristics of geopolymer mortar. *Eng. Sci. Technol. Int. J.* **2017**, *20*, 1642–1652. [[CrossRef](#)]
46. Li, H.; Gao, P.; Xu, F.; Sun, T.; Zhou, Y.; Zhu, J.; Peng, C.; Lin, J. Effect of Fine Aggregate Particle Characteristics on Mechanical Properties of Fly Ash-Based Geopolymer Mortar. *Minerals* **2021**, *11*, 897. [[CrossRef](#)]
47. Şahin, F.; Uysal, M.; Canpolat, O. Systematic evaluation of the aggregate types and properties on metakaolin based geopolymer composites. *Constr. Build. Mater.* **2021**, *278*, 122414. [[CrossRef](#)]
48. Sreenivasulu, C.; Guru, J.J.; Sekhar, R.M.V.; Pavan, K.D. Effect of fine aggregate blending on short-term mechanical properties of geopolymer concrete. *Asian J. Civ. Eng.* **2016**, *17*, 537–550.
49. Embong, R.; Kusbiantoro, A.; Shafiq, N.; Nuruddin, M.F. Strength and microstructural properties of fly ash based geopolymer concrete containing high-calcium and water-absorptive aggregate. *J. Clean. Prod.* **2016**, *112*, 816–822. [[CrossRef](#)]
50. Provis, J.L.; Hajimohammadi, A.; Rees, C.A.; Van Deventer, J.S.J. Analysing and manipulating the nanostructure of geopolymers. In *Nanotechnology in Construction 3*; Springer: Berlin/Heidelberg, Germany, 2009; pp. 113–118.
51. Khedmati, M.; Alanazi, H.; Kim, Y.-R.; Nsengiyumva, G.; Moussavi, S. Effects of Na₂O/SiO₂ molar ratio on properties of aggregate-paste interphase in fly ash-based geopolymer mixtures through multiscale measurements. *Constr. Build. Mater.* **2018**, *191*, 564–574. [[CrossRef](#)]

52. Luan, C.; Shi, X.; Zhang, K.; Utashev, N.; Yang, F.; Dai, J.; Wang, Q. A mix design method of fly ash geopolymer concrete based on factors analysis. *Constr. Build. Mater.* **2021**, *272*, 121612. [[CrossRef](#)]
53. Xie, T.; Visintin, P.; Zhao, X.; Gravina, R. Mix design and mechanical properties of geopolymer and alkali activated concrete: Review of the state-of-the-art and the development of a new unified approach. *Constr. Build. Mater.* **2020**, *256*, 119380. [[CrossRef](#)]
54. Nikoloutsopoulos, N.; Sotiropoulou, A.; Kakali, G.; Tsvivilis, S. Physical and Mechanical Properties of Fly Ash Based Geopolymer Concrete Compared to Conventional Concrete. *Buildings* **2021**, *11*, 178. [[CrossRef](#)]
55. Peng, Y.; Unluer, C. Analyzing the mechanical performance of fly ash-based geopolymer concrete with different machine learning techniques. *Constr. Build. Mater.* **2022**, *316*, 125785. [[CrossRef](#)]
56. Pouhet, R.; Cyr, M. Formulation and performance of flash metakaolin geopolymer concretes. *Constr. Build. Mater.* **2016**, *120*, 150–160. [[CrossRef](#)]
57. Hassan, A.; Arif, M.; Shariq, M. Age-dependent compressive strength and elastic modulus of fly ash-based geopolymer concrete. *Struct. Concr.* **2020**, *23*, 473–487. [[CrossRef](#)]
58. Ojha, A.; Aggarwal, P. Fly ash based geopolymer concrete: A comprehensive review. *Silicon* **2021**, *14*, 2453–2472. [[CrossRef](#)]
59. Joseph, B.; Mathew, G. Influence of aggregate content on the behavior of fly ash based geopolymer concrete. *Sci. Iran.* **2012**, *19*, 1188–1194. [[CrossRef](#)]
60. Albidah, A.; Alghannam, M.; Abbas, H.; Almusallam, T.; Al-Salloum, Y. Characteristics of metakaolin-based geopolymer concrete for different mix design parameters. *J. Mater. Res. Technol.* **2021**, *10*, 84–98. [[CrossRef](#)]
61. Guades, E.J. Effect of coarse aggregate size on the compressive behaviour of geopolymer concrete. *Eur. J. Environ. Civ. Eng.* **2019**, *23*, 693–709. [[CrossRef](#)]
62. Fazli, H.; Yan, D.; Zhang, Y.; Zeng, Q. Effect of Size of Coarse Aggregate on Mechanical Properties of Metakaolin-Based Geopolymer Concrete and Ordinary Concrete. *Materials* **2021**, *14*, 3316. [[CrossRef](#)] [[PubMed](#)]
63. Pan, Z.; Sanjayan, J.G.; Kong, D.L.Y. Effect of aggregate size on spalling of geopolymer and Portland cement concretes subjected to elevated temperatures. *Constr. Build. Mater.* **2012**, *36*, 365–372. [[CrossRef](#)]
64. Li, N.; Shi, C.; Zhang, Z.; Wang, H.; Liu, Y. A review on mixture design methods for geopolymer concrete. *Compos. Part B Eng.* **2019**, *178*, 107490. [[CrossRef](#)]
65. Osuji, S.O.; Inerhunwa, I. Determination of optimum characteristics of binary aggregate mixtures. *Civ. Environ. Res.* **2015**, *7*, 68–75.
66. Davidovits, J. *Geopolymer Chemistry and Applications*, 3rd ed.; Davidovits, J., Ed.; Institut Géopolymère: Saint-Quentin, France, 2011.
67. ASTM C33/C33M-16e1; Standard Specification for Concrete Aggregates. ASTM International: West Conshohocken, PA, USA, 2016.
68. Al Salaheen, M.; Alaloul, W.S.; Malkawi, A.B.; de Brito, J.; Alzubi, K.M.; Al-Sabaeei, A.M.; Alnarabiji, M.S. Modelling and Optimization for Mortar Compressive Strength Incorporating Heat-Treated Fly Oil Shale Ash as an Effective Supplementary Cementitious Material Using Response Surface Methodology. *Materials* **2022**, *15*, 6538. [[CrossRef](#)]
69. Nuruddin, M.; Malkawi, A.; Fauzi, A.; Mohammed, B.; Al-Mattarneh, H. Effects of alkaline solution on the microstructure of HCFA geopolymers. *Eng. Chall. Sustain. Future* **2016**, *501*, 501–505.
70. Neville, A.M. *Properties of Concrete*, 5th ed.; Prentice Hall Pearson: Harlow, UK, 2011.
71. ASTM C192/C192M-16a; Standard Practice for Making and Curing Concrete Test Specimens in the Laboratory. ASTM International: West Conshohocken, PA, USA, 2016.
72. EN 12390-3; Testing hardened concrete—Part 3: Compressive strength of test specimens. BSI: London, UK, 2019; p. 8.
73. ASTM C143/C143M-15a; Standard Test Method for Slump of Hydraulic-Cement Concrete. ASTM International: West Conshohocken, PA, USA, 2015.
74. C231/C231M-17a; Standard Test Method for Air Content of Freshly Mixed Concrete by the Pressure Method. American Society of Testing and Materials: West Conshohocken, PA, USA, 2017; pp. 1–10.
75. ASTM C642-13; Standard Test Method for Density, Absorption, and Voids in Hardened Concrete. ASTM International: West Conshohocken, PA, USA, 2013.
76. Elzokra, A.A.E.; Hourri, A.A.; Habib, A.; Habib, M.; Malkawi, A. Shrinkage Behavior of Conventional and Nonconventional Concrete: A Review. *Civ. Eng. J.* **2020**, *6*, 1839–1851. [[CrossRef](#)]
77. Lie, H.A.; Gan, B.S.; Suryanto, B.; Priastiwi, Y.A. Influence of the stiffness modulus and volume fraction of inclusions on compressive strength of concrete. *Procedia Eng.* **2017**, *171*, 760–767. [[CrossRef](#)]
78. Luo, Z.; Li, W.; Wang, K.; Castel, A.; Shah, S.P. Comparison on the properties of ITZs in fly ash-based geopolymer and Portland cement concretes with equivalent flowability. *Cem. Concr. Res.* **2021**, *143*, 106392. [[CrossRef](#)]
79. Luo, Z.; Li, W.; Wang, K.; Shah, S.P.; Sheng, D. Nano/micromechanical characterisation and image analysis on the properties and heterogeneity of ITZs in geopolymer concrete. *Cem. Concr. Res.* **2022**, *152*, 106677. [[CrossRef](#)]
80. 211.4R-93; Guide for Selecting Proportions for High-Strength Concrete with Portland Cement and Fly Ash. Technical Documents; American Concrete Institute: Farmington Hills, MI, USA, 1998.

Disclaimer/Publisher's Note: The statements, opinions and data contained in all publications are solely those of the individual author(s) and contributor(s) and not of MDPI and/or the editor(s). MDPI and/or the editor(s) disclaim responsibility for any injury to people or property resulting from any ideas, methods, instructions or products referred to in the content.